The Design and Implementation of an Endoscopic Enabled Mouth Gag

---

A Thesis Presented to the Faculty of the Graduate School

University of Missouri – Columbia

In Partial Fulfillment

of the Requirements for the Degree

Master of Science

By

Josh Lewis

Dr. Hao Li, Thesis Supervisor

July 2016

The undersigned, appointed by the dean of the Graduate School, have examined the thesis or dissertation entitled

The Design and Implementation of an Endoscopic Enabled Mouth Gag

presented by Josh Lewis,

a candidate for the degree of Master of Science,

and hereby certify that, in their opinion, it is worthy of acceptance.

Professor Hao Li

Professor Yuyi Lin

Professor Eliav Gov-Ari

Dedication

This thesis is dedicated to my loving wife Crystal for her unconditional support throughout my graduate studies.

Acknowledgements

I would like to express my gratitude to Dr. Hao Li for granting me the opportunity to be a part of this project. His expertise, insight into the medical device industry, and patience were invaluable to the success of this project.

I would also like to thank my committee members: Dr. Yuyi Lin and Dr. Eliav Gov-Ari. Their generous donation of their time and energy were integral in this study. They have proven time and again to support me in any way that they can.

Additionally, I would like to thank Dr. Richard Lebens, Dr. Andrew Ritts, Brian Rader, Zhifeng Lu, Dr. Jaya Ghosh, and Dr. Cynthia Helphingstine for their assistance and kindness.

Table of Contents

List of Illustrations

Figure **Page**

List of Tables

Table **Page**

List of Abbreviations

Abbeviation	Meaning
EEMG	Endoscopic Enabled Mouth Gag
MMO	Maximum Mouth Opening

The Design and Implementation of an Endoscopic Enabled Mouth Gag

Josh Lewis

Dr. Hao Li, Thesis Advisor

Abstract

The purpose of this project was to design and produce a working prototype of a device that could be used in upper airway Otolaryngology surgeries to increase nasopharynx visualization. The nasopharynx is the anatomical region of the airway that is behind the nose and above the palate, and therefore very difficult for surgeons to access and properly visualize. Traditional methods include the blind removal of diseased tissue or the use of a small, hand-supported, dental-style mirror for visualization during tissue removal with a cutting tool. The blind method is severely limiting for the surgeon. The use of the mirror has advantages over the blind method, but has a restricted field of view and limits the surgeon's ability to visualize the procedure as well. The proposed endoscopic enabled mouth gag (EEMG) device attaches to the traditional mouth gag and allows for the fixation of a rigid endoscope that can be positioned as needed and

locked into place. The improved field of view of the endoscope over the mirror allows for superior visualization for the surgeon. The device was designed using Solidworks, produced using Polyjet 3D printing technology, and tested in conjunction with a Crowe-Davis mouth gag, rigid endoscope and anatomical mannequin for functionality and ease of use.

1. Introduction

The overall goal of my master's study was to design a working prototype of a medical device that could be utilized to assist in Otolaryngology upper airway surgical procedures. The device, named the endoscopic enabled mouth gag (EEMG), allows for the incorporation of a supported and articulable endoscope into the traditional surgical equipment, which provides for superior visualization of the anatomical structures during surgery over traditional methods. Chapter 1 provides background information on the relevant human anatomical structure and the challenges it poses for surgeons, the pathophysiology of the common diseased tissues in this region, surgical methods currently used to remove diseased tissue, and the need for an assistive device to improve upon traditional methods. Chapter 2 describes the details of the design process of such a device and the development and testing of three stages of prototypes.

1.1 Anatomy

The upper airway consists of a continuous path for air to enter through the nose via the nares, or nostrils, and into the lungs. It is divided into the nasal cavity, the larynx, and trachea. The larynx is further subdivided into three sections consisting of the nasopharynx, oropharynx, and laryngopharynx (see Fig. 1.) The nasopharynx extends from the base of the skull, at the Clivus, to the soft palate. The oropharynx extends from the hard palate to the Hyoid bone. And the laryngopharynx extends from the upper region of the Epiglottis to the lower region of the Cricoid cartilage [1]. The nasal cavity is separated from the oral cavity by the hard and soft palate. The soft palate functions as a gate that can close to isolate the oral cavity, preventing solids and liquid from entering the pharynx, usually during eating or drinking. Due to the limited size of the nares, especially in children, and the barrier provided by the palate, the nasopharynx can be a very difficult region to access [1].

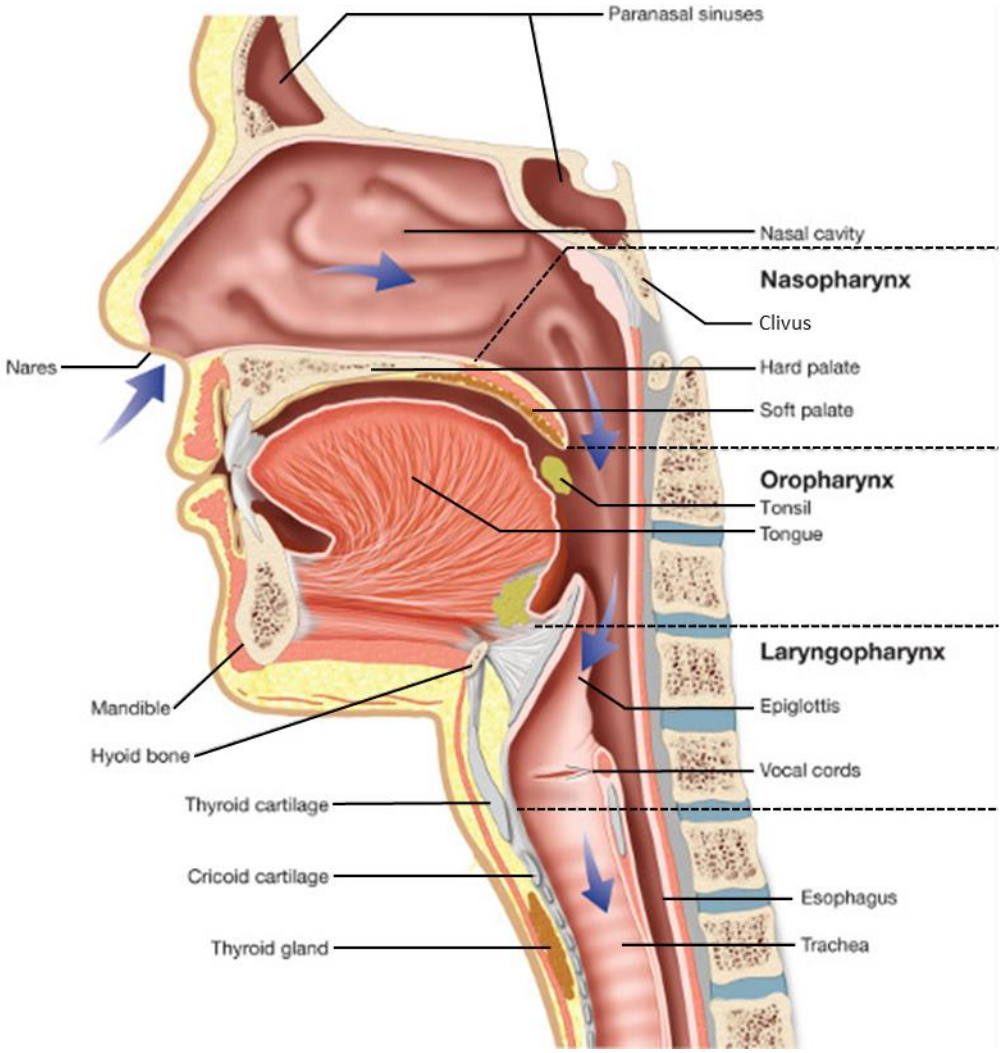

Fig. 1. Sagittal section of upper respiratory system illustrating the internal anatomy of the nasal cavity, pharynx, larynx, and trachea. Reprinted from http://biology-forums.com/index.php?action=gallery;sa=view;id=8486, "6/12/2016".

In addition to serving as a portion of the upper airway, the nasopharynx also houses the adenoids, is the site of the ostium, or opening, of the Eustachian tubes, and is bordered by the Choana (rear nostrils). The adenoids are one of two sets of lymphatic tissue, the other being the tonsils, which comprise the Waldeyer ring [2]. The

adenoids initiate an immune response to airborne antigens entering through the nose, while the tonsils protect against those entering through the mouth [2]. The adenoids are located on the roof of the nasopharynx as can be seen in Fig. 2. The Eustachian tubes are narrow passages connected to the middle ear that open into the nasopharynx, also seen in Fig. 2. They allow for the pressure equalization of the eardrum respective to the ear canal.

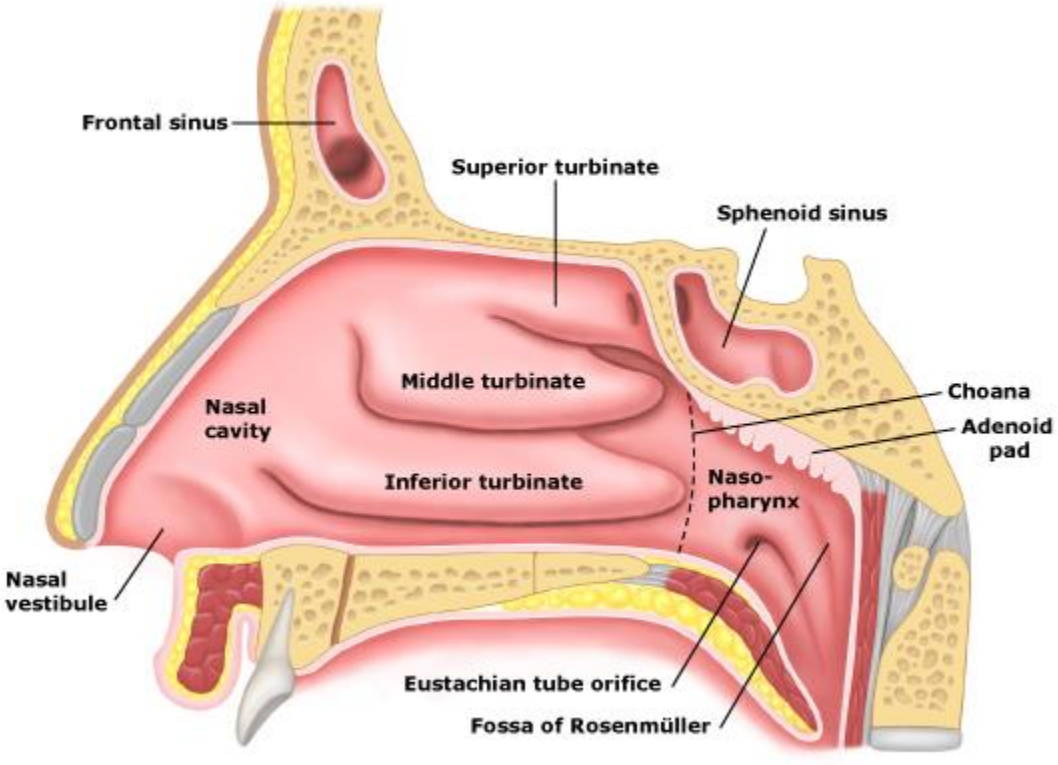

Fig. 2. Sagittal section of upper respiratory system highlighting the adenoids, Eustachian tube ostium, and their respective locations. Reprinted from *Nasopharynx, 2011*, http://www.painneck.com/nasopharynx, "6/12/2016".

1.2 Pathophysiology and Epidemiology

There are several diseases that can occur in the tissues of the nasopharynx that require surgery in this location if severe. Some of these can take the form of growths such as tumors, cysts, and enlarged tissue, or even closed or otherwise restricted orifices. Examples include Clival Chordomas, juvenile nasopharyngeal Angiofibroma, Thornwaldt cysts, enlarged adenoids, Choanal atresia, and Eustachian tube dysfunction. While many of these diseases can be severe and even have high mortality rates, this study will focus on enlarged adenoids, due to the extremely high incidence rate with respect to the other diseases.

The enlargement of the adenoids can come from two separate causes. The first being infection, and the second being increased immunological responses during different periods of early development [3]. By puberty, most adenoids have drastically reduced in size, or disappeared completely [3].

Enlarged adenoids are problematic for two main reasons. The first, being chronic nose, throat, or ear infections, and the second being obstructive breathing. The adenoid is designed to trap bacteria and other antigens, and subsequently becomes infected. These infections spread to the surrounding areas of the nasal cavity,

Eustachian tubes, and oropharynx. Additionally, the enlargement of the adenoids reduces the size of the airway.

It has been shown that Poiseuille's Law can be used to characterize the relation between the flow rate though the airway and the airway radius [4]. Poiseuille's law, described in Eqs (1-3) and Fig. 3., shows that the volumetric flow rate through a tube is proportional to the pressure differential between the inlet and outlet, and the forth power of the tube radius, and inversely proportional to the tube length. The consequences of this are evident if the pressure differential and the tube length are held constant, and the tube diameter is changed by a small amount. For example, if the radius of the tube is halved, the volumetric flow rate will be reduced to $1/16^{th}$. This is often the case with enlarged adenoids, as they are commonly observed to obstruct the airway upwards of 50%. Subsequently, adenoidectomy has become common practice to combat obstructive sleep apnea syndrome [5].

$$Q = \frac{P_1 - P_2}{R} \quad (1)$$

$$R = \frac{8\eta L}{\pi r^4} \quad (2)$$

$$Q = \frac{(P_1 - P_2)\pi r^4}{8\eta L} \quad (3)$$

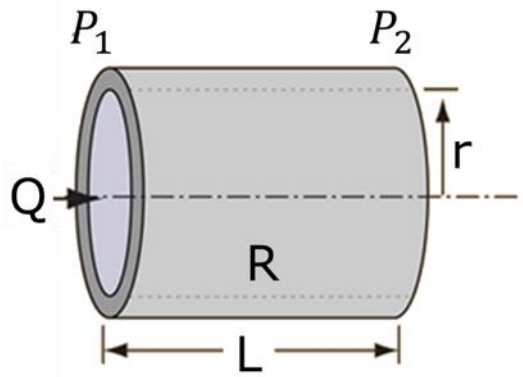

Fig. 3. Illustration depicting the parameters concerning Poiseuille's Law. Reprinted from Nave R., *Poiseuille's Law*, http://hyperphysics.phy-astr.gsu.edu/hbase/ppois.html, "6/12/2016".

Q = Volumetric Flow Rate

R = Resistance to Flow

P1 = Pressure at inlet

P1 = Pressure at outlet

L = Length

r = radius

η = Viscosity of Fluid

In 2006 over 636,000 adenoidectomies with or without tonsillectomy were performed in the US, a 66.6% increase over the previous decade [6]. The mean age for adenoidectomy is 6 years old [6]. The most common complication resulting from adenoidectomies is post-operative bleeding, with rates observed as high as 10% [2], and mortality is estimated between 1:16,000 and 1:35,000 [2].

1.3 Surgical Methods and Clinical Need

In a traditional adenoidectomy procedure, the patient is put under anesthesia, intubated, and immobilized laying down, face up. The soft palate is retracted using two rubber catheters, one entering each nostril, proceeding through the nasal cavity, nasopharynx, and out the oral cavity, where the ends are secured. A Crowe-Davis mouth gag frame is positioned over the patient's mouth, with the top teeth in the teeth tray. A tongue blade is positioned into the mouth above the tongue and breathing tube. The tongue blade handle is inserted into the mouth gag frame handle, and the pulled towards the patient's chest to extend the jaw. The ratcheting mechanism on the mouth gag frame secures the tongue blade until the release lever is depressed.

Several surgical methods are used for dissection of the adenoids. These consist of cold dissection, electrocautery, coblation, and microdebrider. Cold dissection is the most traditional method for adenoidectomies, using a curette in a blind manner, or scalpel with mirror to cut the adenoids from the surrounding tissue [2]. Electrocautery uses electrical resistance to generate localized temperatures up to 600° C in the adenoid tissue to remove it from the surrounding tissue, and has the added benefit of providing hemostasis during dissection [2]. Coblation uses an ionized plasma field break the molecular bonds to dissolve the adenoid tissue and has been shown to reduce thermal damage to surrounding tissue over electrocautery [2]. In both electrocautery and coblation, a mirror is generally used for visualization. The microdebrider technique uses a blade spinning at a high rate to excise tissue, which is then suctioned for removal [2]. This method allows for precise cuts, but requires a high degree of visualization to do so.

Despite the surgical method used, the success of the procedure is dependent upon the surgeon's ability to visualize the tissue to be removed and that surrounding it. This has been demonstrated in a comparison of surgical methods differing in their level of visualization, and recounted by Otolaryngology residents first hand.

A study was conducted by Anand, V. et al, compared 40 pediatric adenoidectomy cases of age group 3-14 year, 20 performed with the traditional method of blind curette (Group A), and 20 performed with endoscopic assisted microdebrider (Group B) [7]. The metrics of comparison included intra-operative time, primary bleeding, completeness of removal, and post-operative pain and recovery. The results of the study showed that the endoscopic assisted microdebrider approach was significantly more successful in every metric. Group A had a mean intra-operative time of 16 min. and 20 sec., while that of Group B was 12 min. and 10 sec. Group A had primary bleeding of 40 ml., while that of Group B was 35 ml. Group A had 75% of cases with complete tissue removal and 25% of cases with partial tissue removal, while Group B had 100% complete tissue removal. Group A had 45% of cases score a 5, 35% score a 4, and 20% score a 6 on the Hanallah Objective Pain Scale, while Group B had 70% score a 4, 25 % score a 5, and 5% score a 3 on the same scale. Group A had 70% of cases recover within 4 days, and 30% within 5 days, while Group B had 85% recover within 4 days, and 15% recover within 3 days. The study contributed the success of the endoscopic assisted microdebrider method to the superior visualization provided by the endoscope, as surrounding tissue is not damaged and complete removal of the tissue is guaranteed.

In interviews with University of Missouri Otolaryngology residents (year 1-5), the need for improved visualization over traditional methods was heavily stressed [8]. Through talking with these individuals, it became apparent that even with the mirror assisted electrocautery and coblation methods, that the use of an endoscope would greatly improve their ability to become proficient performing adenoidectomies and the outcomes of such procedures.

While a resident is learning this procedure it is very difficult to observe the instructor performing the surgery, as direct line of sight to the nasopharynx is only provided to the individual performing the surgery. This results in significant verbal description of the surgeon's actions, and the resident has to use their knowledge of the anatomy and their imagination to follow. Additionally, when the resident attempts to perform the surgery, the instructor cannot monitor their actions. This severely limits the instruction and quality control of adenoidectomies in a teaching hospital setting. As 76.8% of adenoidectomies are performed in teaching hospitals [9], a superior visualization technique could have a large impact. All those interviewed agreed that the incorporation of an endoscope into the procedure for visualization would improve their ability to learn the procedure.

Through the case presented above and direct correspondence with Otolaryngology residents, it is apparent that traditional methods for visualizing adenoidectomy surgery, despite the method, are inferior to that provided by the assistance of an endoscope.

2. Device Design

The goal of this study was to design and produce a working prototype of the EEMG device. The purpose of this device would be to provide superior visualization and easy access to the relevant anatomical structures over traditional methods for Otolaryngology procedures performed in the nasopharynx, by the incorporation of a supported endoscope. The device would be consistent with the description of such a device by Dr. Eliav Gov-Ari and Alex Maddinger, as outlined in the international application published under the Patent Cooperation Treaty, application number PCT/US2014/057768.

To accomplish the end goal of a fully functioning device, three prototype stages were proposed. The first prototype would have three basic requirements. The first being that it would incorporate the Crowe-Davis mouth gag. The second requirement would be to provide the basic range of motion required of the endoscope for a surgical

procedure in the Nasopharynx. And the final requirement of the first prototype would be to provide the basic functionality to lock and secure the camera and endoscope in position. The second prototype stage would have two requirements. The first being to successfully address any issues that should arise during first stage testing of range of motion and functionality. The second requirement of this prototype would be to provide features to incorporate the camera and endoscope in a removable fashion and also any supporting operating room equipment. The third prototype stage would have two requirements. The first requirement would be to address any issues that should arise during second stage testing. The second requirement of this final stage prototype would be to incorporate features that would allow the device to quickly and easily attach to the mouth gag frame. If all requirements from the three prototype stages could be met, the overall goal of a fully functional EEMG device would be satisfied for this project.

2.1 Concept

The concept of the EEMG is that of a device consisting of three main parts: (1) a Crowe-Davis style mouth gag, (2) a tongue blade, and (3) an adjustable endoscopic support structure, as can be seen in Fig. 4. The endoscopic support structure consists of four main components. The first being a scope holder member, which holds the endoscope/camera assembly. The second being a main telescoping shaft attached at one end to the mouth gag frame and at the other to the endoscope/camera assembly holder. At both ends of this main shaft are lockable ball-socket joints that, when combined with the telescoping motion of the shaft, provide for six degrees of freedom of the endoscope/camera assembly. The third are the secondary support shafts, which attach, by freely rotating, snap-fit, ball-socket joints, to the upper and lower sections of the main shaft at one end, and to the fourth member, the front support cross-bar, at the other end. The front support cross-bar attaches to the mouth gag frame where it would contact the lower jaw. These last members provide additional support of the endoscope/camera and stabilize the base.

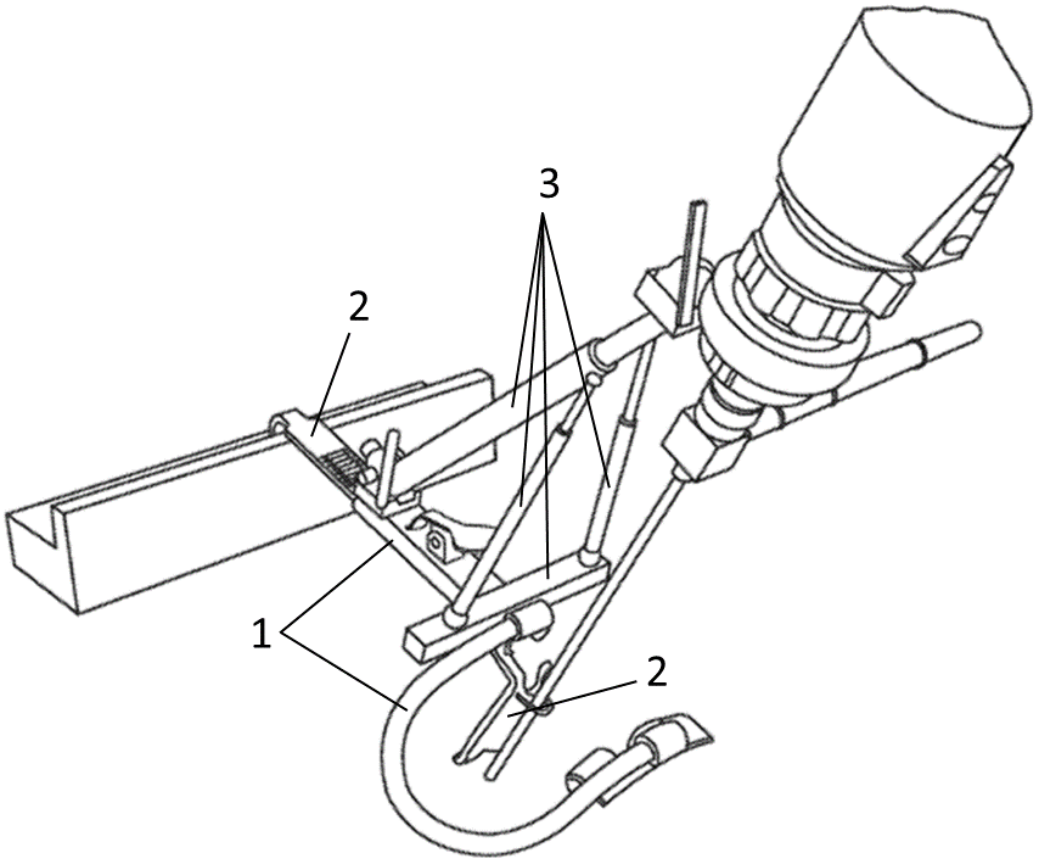

Fig. 4. Illustration of the EEMG components form patent. Reprinted from Gov-Ari, E., Maddinger, A., (2015), Endoscopic-Enabled Mouth Gag and Associated Method of Use.

To use the device, six basic steps are required. First, the main shaft and the front support cross-bar are attached to the mouth gag frame. Second, the mouth gag is put into place on the patient as in a traditional surgical procedure for an adenoidectomy. Third, the secondary support shafts are attached by snapping the balls into the sockets. Fourth, the main shaft locking levers are toggled off and the support structure is articulated into approximate position. Fifth, the endoscope/camera assembly is inserted into the scope holder. Sixth,

the support structure is articulated into exact position and the main shaft locking levers are toggled on, fixing the endoscope/camera assembly in place. The entire process taking approximately 30 additional seconds to complete over the setup process of an adenoidectomy. To remove the device, the above steps are simply reversed. At any point, the endoscope/camera assembly may be easily removed from the device as needed for cleaning or if traditional methods are to be used mid-surgery.

2.2 Prototype Manufacturing

For prototype production, 3D printing (additive manufacturing) was chosen for time and cost effectiveness over traditional manufacturing methods. Although there are many different 3D printing methods with widely different technologies, the basic concept is similar. 3D CAD software is used to design and create a 3D model of the part to be printed. The part file is divided into horizontal layers in a process called slicing, just as if you were to divide an orange by slicing it with a knife and then continue to make several parallel slices all the same distance apart from one another. Stacked in the proper order and bonded together, the layers build the whole orange. The individual part slices represent layers that can be manufactured one at

a time, usually from the bottom of the part up, and bonded to the layer beneath to build the whole part.

The University of Missouri Prototype Development Facility is associated with the College of Engineering and provides priority 3D printing services at the cost of materials to students. Additionally, the site is located at Mizzou North, just two miles from the College of Engineering. With the priority service and close proximity, same day service was often available for the production of parts for this project. This allowed for quick testing of parts for fit and functionality, and coupled with the low cost of production, design changes could be highly iterative. Whereas, traditional manufacturing methods would have had lead times of weeks before parts could be produced and tested. Additionally, the cost would have been much higher due to the labor involved with less automated processes.

Of the many 3D printing services that the University of Missouri Prototype Development Facility offers, Stratasys Polyjet technology was chosen for its high print resolution, rigid print material, available support material, and smooth surface finish. The available Polyjet machine was the Eden 350V (see Fig. 5). The prototype design was anticipated to have many mating parts that would require a fair amount of precision to fit together with the proper clearances. As such, a high print resolution technology would be necessary. The

Objet Eden 350V has a XY print resolution of 600 dpi (0.042 mm) and a Z resolution of 1600 dpi (0.016 mm layer thickness) [10]. Also, although the prototype would ultimately have to support only a small load consisting of the lightweight camera and endoscope, it was a crucial design requirement that the device maintain accurate positioning of the scope. This required the prototype to be relatively rigid to reduce the bending of the members and the subsequent translation of the scope, so a rigid print material would be necessary. Another important requirement of the print technology would be the availability of support material. Without support material, the geometry of the design would be severely limited. Additionally, smooth surface finish was desired for the prototype parts as there would be members that would slide with respect to one another and rough texture would hinder this motion. With these needed characteristics, all parts were printed on the Objet Eden 350V Polyjet machine as it satisfied all conditions.

Fig. 5. Stratasys Objet Eden 350V Polyjet 3D Printer with print head and bed exposed. Reprinted from https://commons.wikimedia.org/wiki/File:Objet_Eden_350_3d_printer.jpg, 6/12/2016".

Polyjet technology has similar preprocessing to standard 3D printing technologies. Once the part is designed, the file is exported to the universal STL file format. The STL file is imported into the Objet software where the model file is sliced into horizontal layers representing the layers to be printed. The software then uses these layers to calculate the XY positions where the print material and

support material are to be placed for each layer [11]. Support material is necessary for overhanging part features that otherwise would not have existing support from the previous layer beneath at that location.

The concept of the production of the 3D printed part with Polyjet technology is similar as well, only differentiated by the material, the way it is distributed and solidified. The Objet Eden 350V Polyjet 3D printer uses a photopolymer print material to build the parts. This is a liquid polymer that cross-links (cures) when exposed to UV light, resulting in a solidified material. The Objet software takes the XY position of each constituent point to be printed for the layer and the support material for that layer, calculated in preprocessing, and the print head (similar to an inkjet printer) translates in this plane to distribute small droplets of the liquid photopolymer material, and separately the support material, at these points [11]. As the print head translates, the UV bulbs attached cure the material just distributed, fusing the droplets together to build the layer as it moves and binding it to the layer beneath. In the case of the first layer, the material is printed directly on the print bed of the machine. Once the current layer has finished, the print head translates in the Z direction by the specified layer thickness and continues the process for the next

print layer. This is repeated until the part is complete. The part is then easily removed from the print bed using a spatula.

Post-processing is simple and requires only that the support material, be cleaned from the part. The support material is water soluble, which helps with the cleaning. The part is generally soaked in water for 10-15 minutes to allow the support material to absorb water and soften. Then the part is power washed with pressurized water. And finally, the part is cleaned using soap and water with an abrasive sponge. In the case of deep holes and orifices, small pieces of stainless steel wire and nylon tube brushes help to dislodge any support material.

As 3D printing was chosen for the prototype development manufacturing method and 3D printing technology is relatively new and quickly changing, guidelines for basic design principles were needed to ensure proper functionality of device components after production and proper mates between components. For a first prototype, that will be used to test for form and function, 3D Matters [12] suggests a minimum wall thickness of 2 mm for all parts. It is also suggested for mating shafts and holes under 25 mm in diameter to use a starting radial clearance of 0.125 mm. And for sliding surfaces, to use a gap clearance of 0.25-0.50 mm. These

recommendations were generally adhered to as design guidelines where possible.

2.3 Prototype 1

The first prototype stage would have three basic requirements to progress on to the final goal of a fully functioning device. The first being that it would incorporate the Crowe-Davis mouth gag. The second requirement would be to provide the basic range of motion required of the endoscope for a surgical procedure in the Nasopharynx. And the final requirement of the first prototype would be to provide the basic functionality to lock and secure the camera and endoscope in position.

2.3.1 Measurements for Basic Dimensions and Range of Motion

In order to obtain an initial estimate of the dimensions of the device and its needed range of motion, several measurements would have to be taken from different sources. These included a Crowe-Davis mouth gag, a paired tongue blade, an appropriate endoscope, and the oral cavity of an average patient.

To accomplish the first three, an Aesculap OM116R Adult Crowe-Davis mouth gag; an Aesculap N7519L4 tongue blade; and a Karl Storz Hopkins II, 7230-EA, 4mm diameter, 20 mm long, 120° endoscope were obtained and various measurements were taken with a Kobalt 6 in. electronic caliper. Then, 3D models of all three pieces of equipment were created using SolidWorks 2014 for assembly and further analysis (see Fig. 6-9.). Additionally, Alex Maddinger supplied a 3D model of a HD camera that could be used with the endoscope mentioned above for size reference (see Fig. 10.).

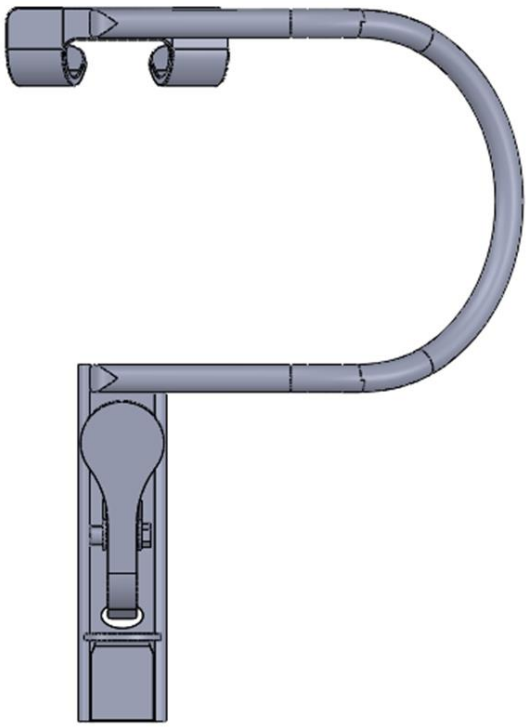

Fig. 6. Aesculap OM116R Adult Crowe-Davis mouth gag 3D model top view.

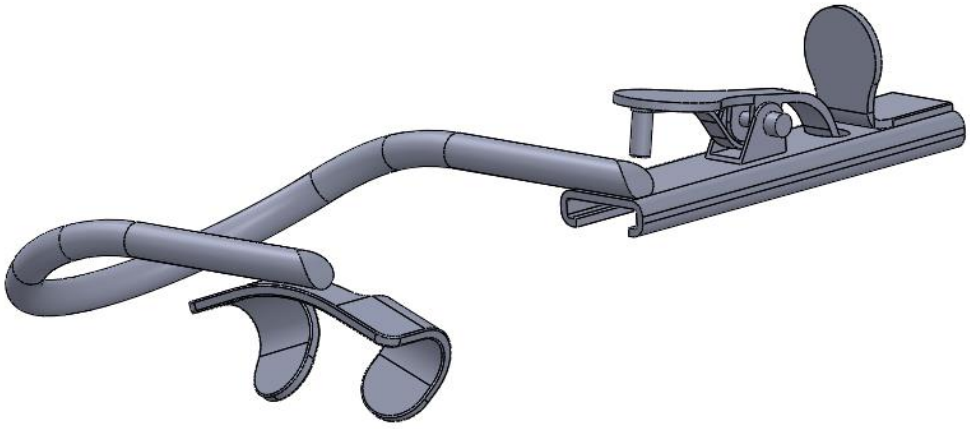

Fig. 7. Aesculap OM116R Adult Crowe-Davis mouth gag 3D model.

Fig. 8. 3D model of Aesculap N7519L4 tongue blade.

Fig. 9. 3D model of Karl Storz Hopkins II, 7230-EA endoscope.

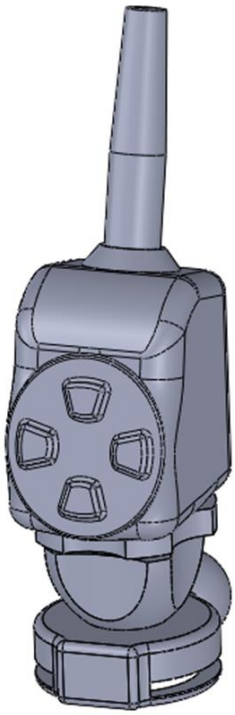

Fig. 10. 3D model of HD camera to be used with the Karl Storz Hopkins II, 7230-EA endoscope.

To obtain an estimate of the average oral cavity dimensions a midline sagittal view CT scan from a healthy adult male was used (see Fig. 11.). This image was scaled using the mean MMO (maximal mouth opening) of 42 mm [13] (corresponding to segment A-B) for the average age adenotonsillar patient of 6 years old [6]. Once scaled, several measurements were made from anatomical landmarks present in the image shown by Points A through E. The first measurement was the maximum depth, as shown by Segment A-D, having the value of approximately 100 mm. This dimension would be the maximum extension of the endoscope into the oral cavity and, knowing the total

length of the endoscope, would give an estimate of the height of the device above the lower surface of the Crowe-Davis mouth gag handle. The second and third were the angle α, having the value of 22.5°, and the angle β, having the value of 27.5°, respectively. The sum of these angles (50°) would be the rotation required of the endoscope to reach any possible point in the nasopharynx, and into the oropharynx if needed.

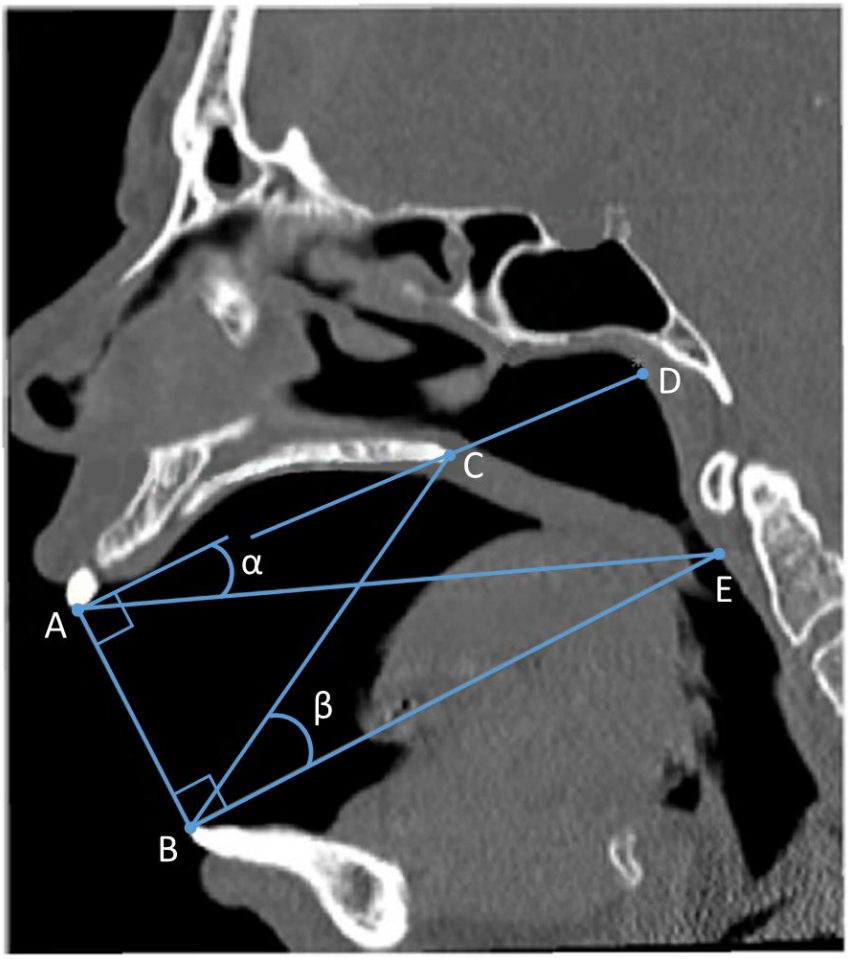

Fig. 11. CT scan of midline sagittal view and landmarks for measurement reference. Reprinted from Amelot A. et al., 2015, "Anatomical features of skull base and oral cavity: a pilot study to determine the accessibility of the sella by transoral robotic-assisted surgery" *Neurosurgical Review*, **38,** 723-730.

Point A: the maxillary dental point at the tip of the superior incisor.

Point B: the mandibular dental point at the tip of the inferior incisor.

Point C: the most posterior palatine bone point.

Point D: the projection of segment A-C onto the posterior of the nasopharynx.

Point E: the projection of Point B perpendicular to Segment A-B onto the posterior of the Oropharynx.

Angle α: angle between Segment A-E and the perpendicular to Segment A-B.

Angle β: angle between Segment B-C and the Segment B-E.

With the basic dimensions of the oral cavity and scope obtained and the models created of the Crowe-Davis mouth gag frame, SolidWorks was used to estimate required range of motion of the main and secondary support shafts. To determine maximum and minimum extensions of the telescoping main shaft and secondary support shafts, two cases were studied. The first being the case of mean MMO for the average adenotonsillar patient. And the second being the maximum MMO possible using the Crowe-Davis mouth gag, measured to be 50 mm.

Using the Crowe-Davis mouth gag frame model, drawings were created with the distal endoscope tip (Point I) at the maximum depth of 100 mm below the lower surface of the mouth gag frame handle (see Fig. 12, 13.). Two endoscope tip positions, forward (I_F) and rear

(I_R), were considered representing the maximum and minimum translation of the vertical endoscope for each case. For each position an approximation of the main shaft length was drawn from the scope holder attachment point of the endoscope (Point H) to the main shaft socket base (Point G). It can be seen from the measurements taken in both cases, shown in Fig. 12, 13., that the maximum extension of the main shaft is 146.44 mm, at an angle of 24.2° from the top horizontal surface of the socket base. And the minimum extension of the main shaft is 106.23 mm, at an angle of 34.5° from the top horizontal surface of the socket base.

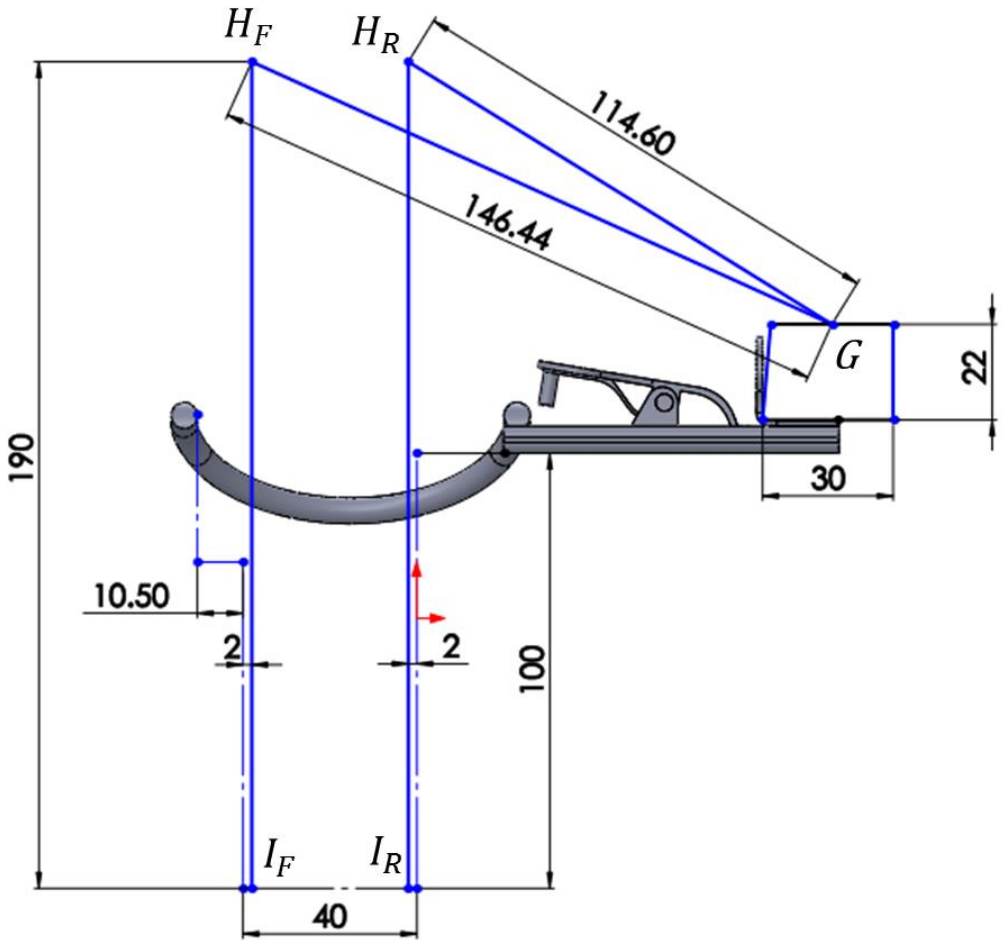

Fig. 12. Mean MMO endoscope tip position, main shaft minimum and maximum extension, and corresponding angles to the horizontal.

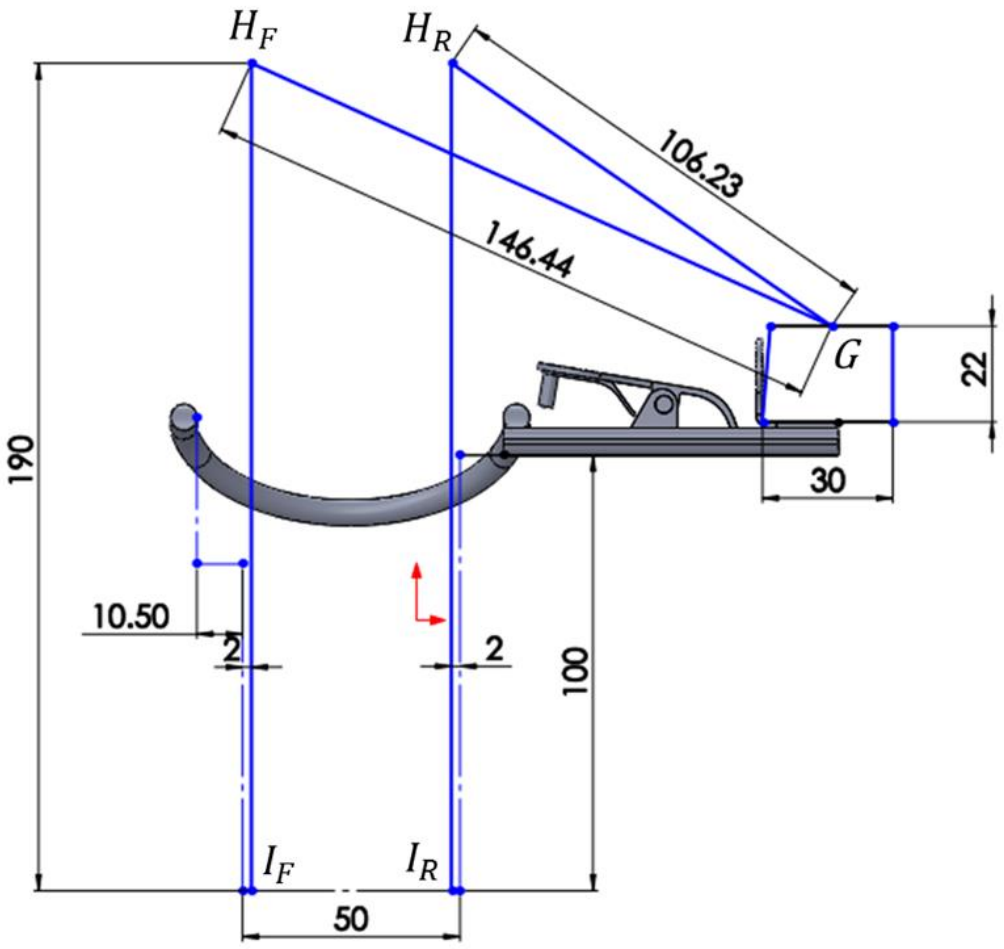

Fig. 13. Maximum MMO endoscope tip position, main shaft minimum and maximum extension, and corresponding angles to the horizontal.

Additionally, similar drawings were made of the secondary support shafts for each case at each endoscope tip position, forward and rear (see Fig. 14-17.). An initial length for the front support cross-bar was chosen to be 110 mm (shown in blue) to provide for adequate stability by taking advantage of the full length of the horizontal portion of the mouth gag frame horseshoe for support. The secondary support shaft length was drawn from the end of the front

support cross-bar (Point J) to Point H. It can be seen from Fig. 14-17., that the maximum extension of the secondary support shaft occurs at the forward position and is the same in either MMO case and is measured to be 115.03 mm. Inspection of the same figures reveals that the minimum extension of the secondary support shaft occurs at the rear position in the maximum MMO case and is measured to be 94.87 mm.

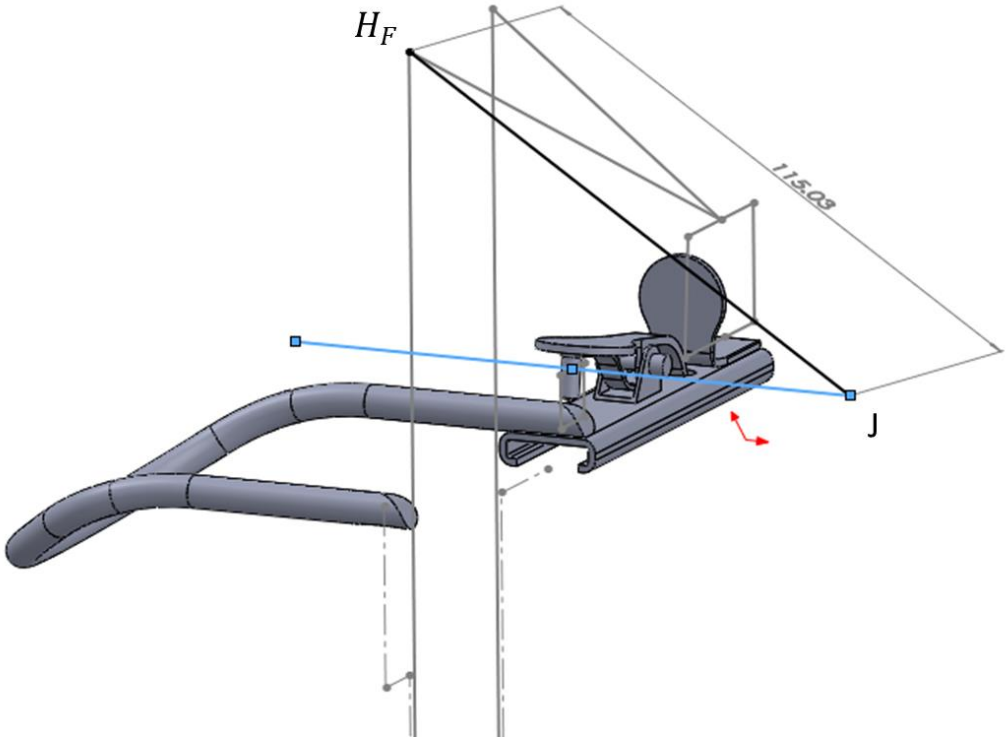

Fig. 14. Mean MMO, forward endoscope tip position, secondary support member maximum extension.

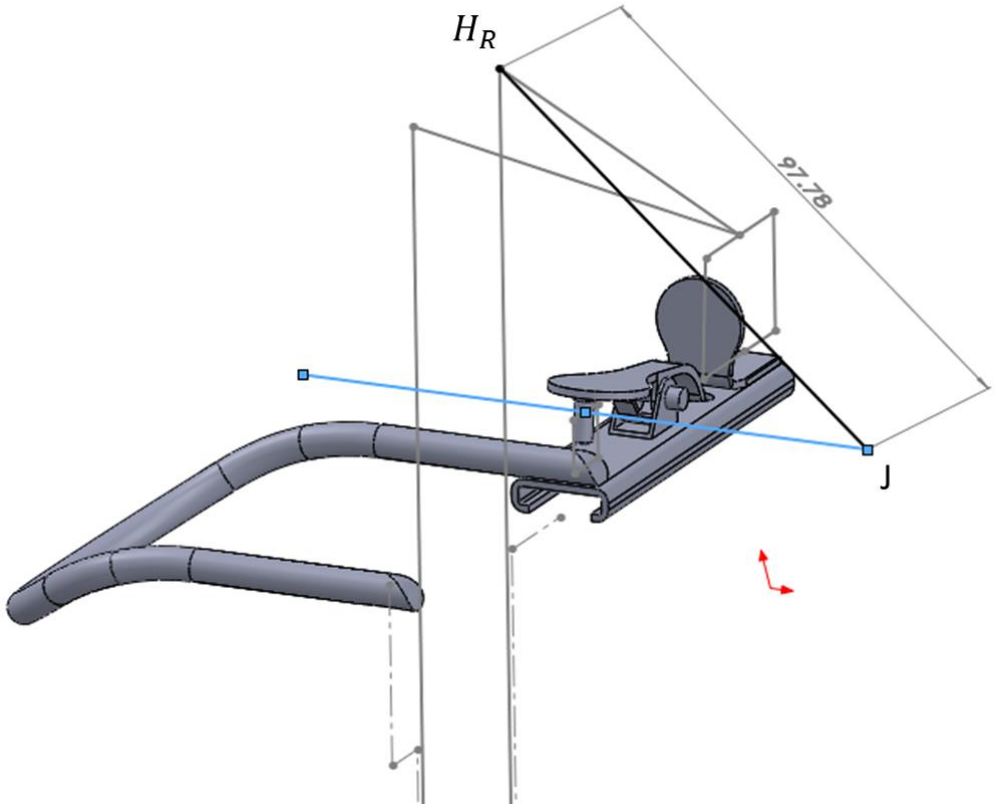

Fig. 15. Mean MMO, rear endoscope tip position, secondary support member minimum extension.

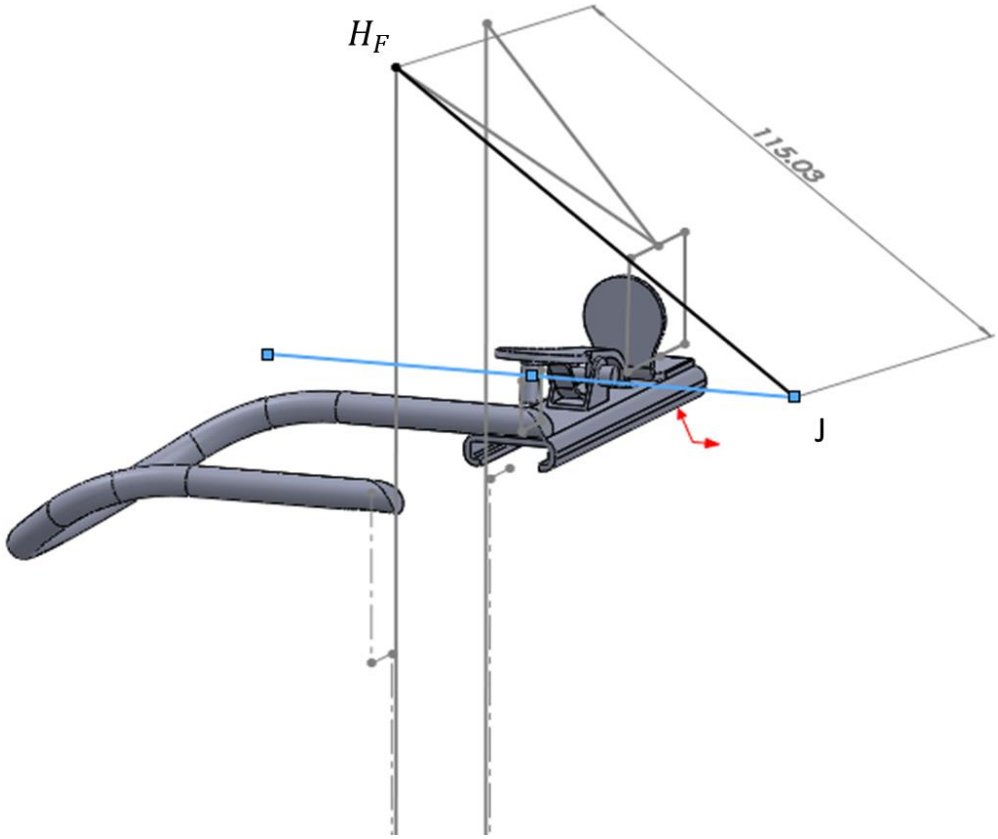

Fig. 16. Maximum MMO, forward endoscope tip position, secondary support member maximum extension.

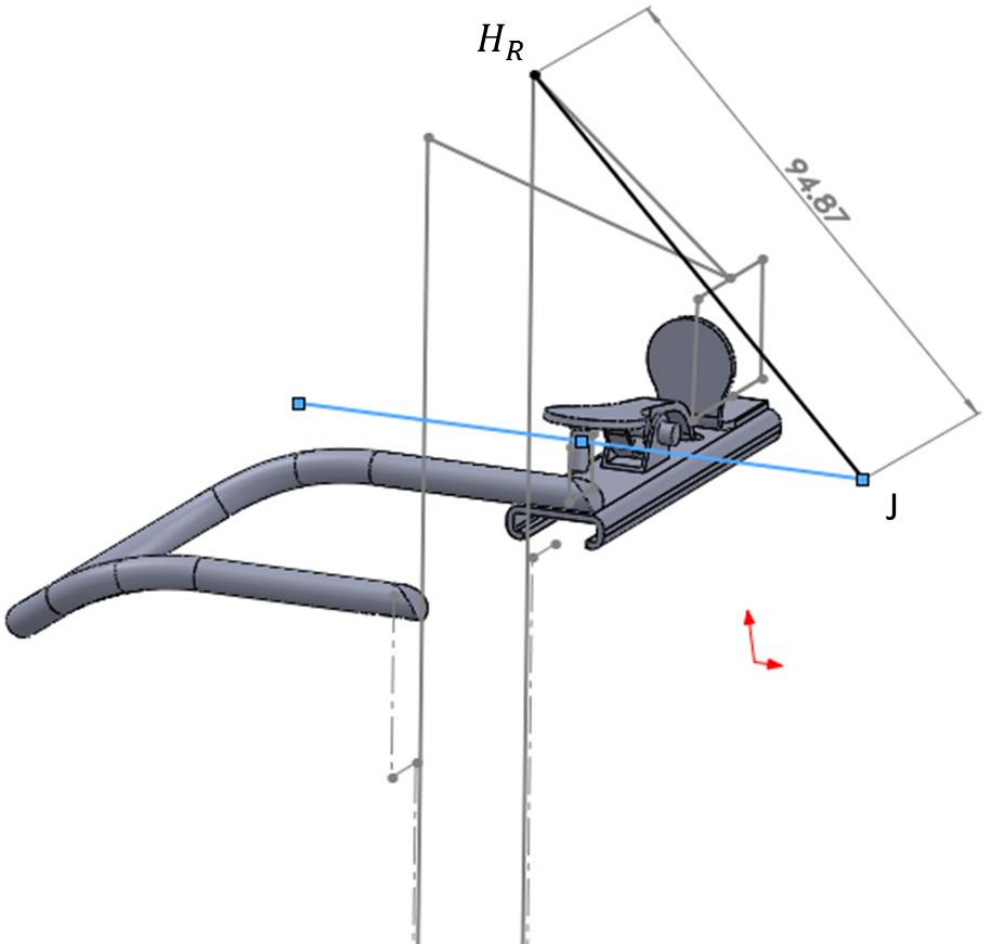

Fig. 17. Maximum MMO, rear endoscope tip position, secondary support member minimum extension.

2.3.2 EEMG Component Design and Function

With the basic EEMG component dimensions and range of motion, SolidWorks was used to build the fundamental models of the components necessary for the support structure of the device. In Fig. 18. these can be seen in green, along with the endoscope/camera assembly in blue, and the traditional Crowe-Davis mouth gag frame and tongue blade in red for reference. These support structure components include the main shaft assembly, the secondary support shafts, the front support cross-bar, and the scope holder. The scope holder in this prototype stage was simplified to be part of the camera itself.

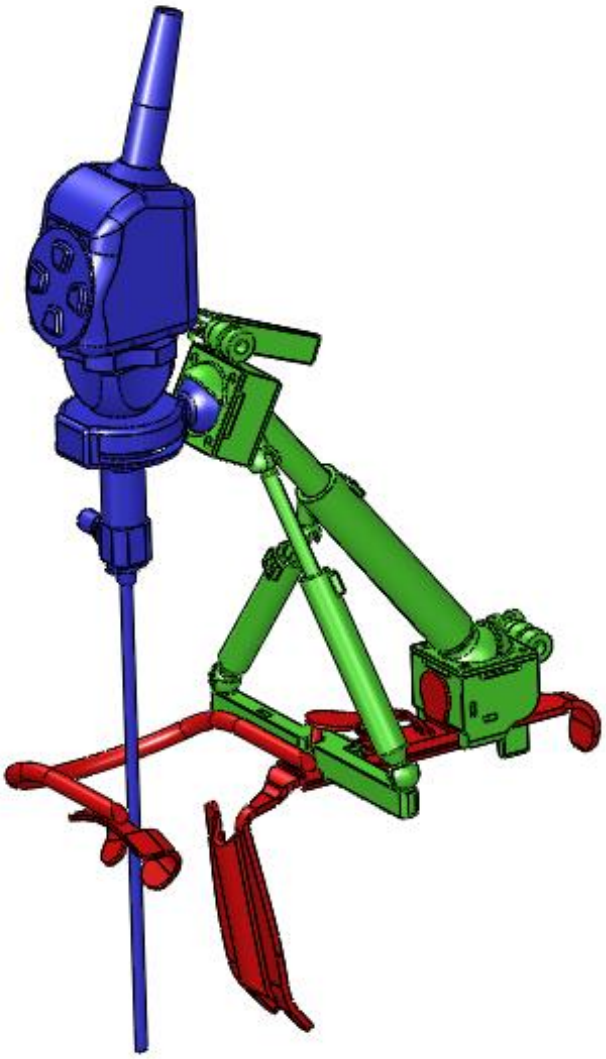

Fig. 18. Assembly of the EEMG prototype 1, consisting of support structure (green), endoscope/camera assembly (blue), and Crowe-Davis mouth gag and tongue blade (red).

The first section of the support structure is the main shaft assembly, which consists of several components (see Fig. 19.). Starting at the base, is the lower locking socket assembly (see Fig. 20.). Next is the main shaft lower cylinder (see Fig. 21.). Last, the

main shaft upper cylinder with upper locking socket assembly (see Fig. 22.).

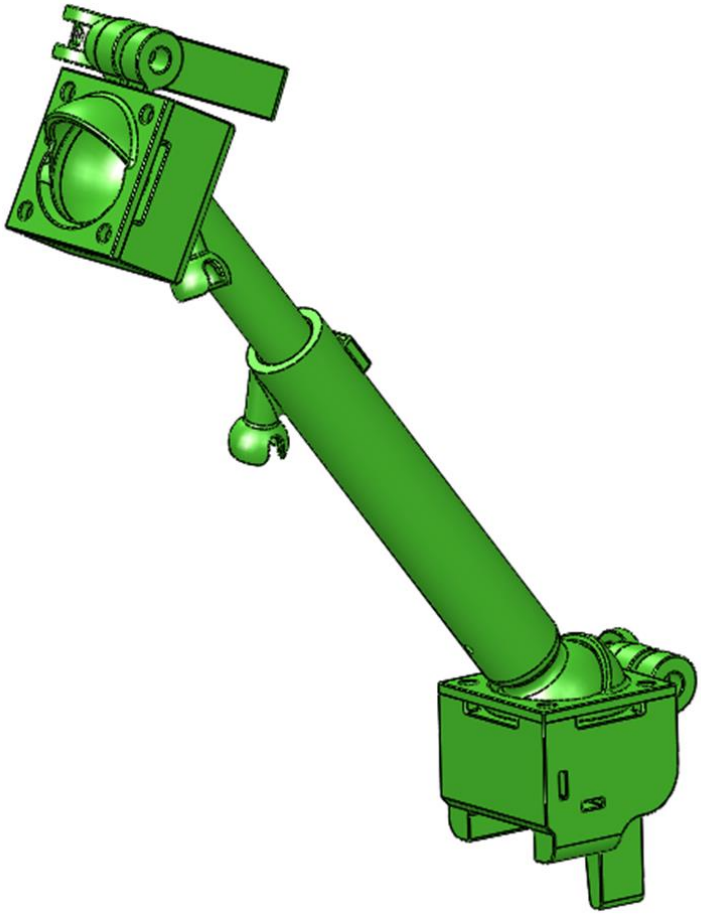

Fig. 19. EEMG support structure main shaft assembly.

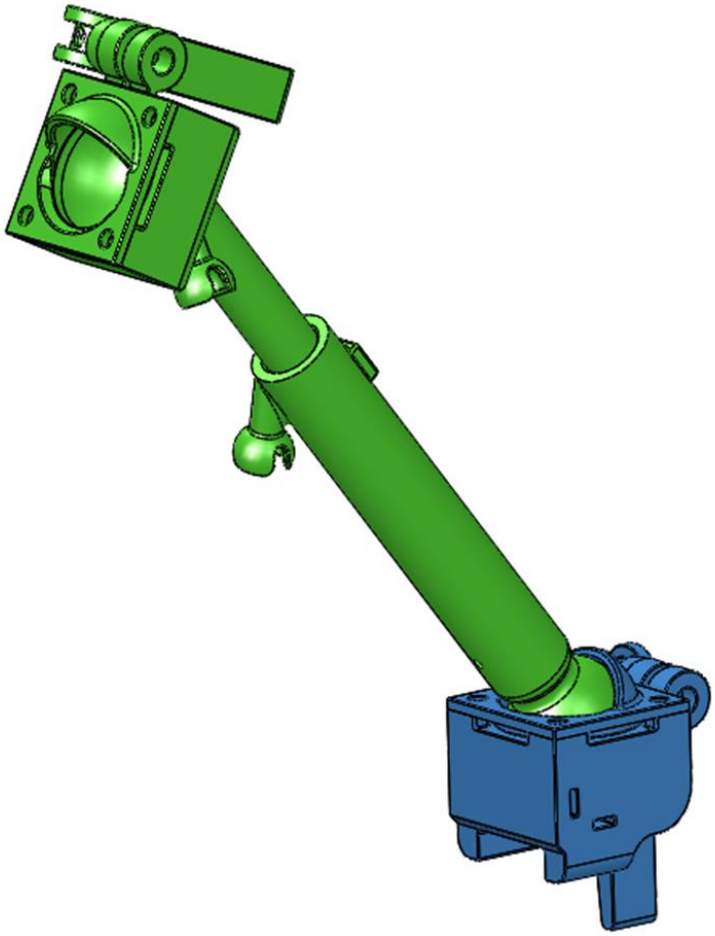

Fig. 20. EEMG support structure main shaft assembly, highlighting the lower locking socket assembly (blue).

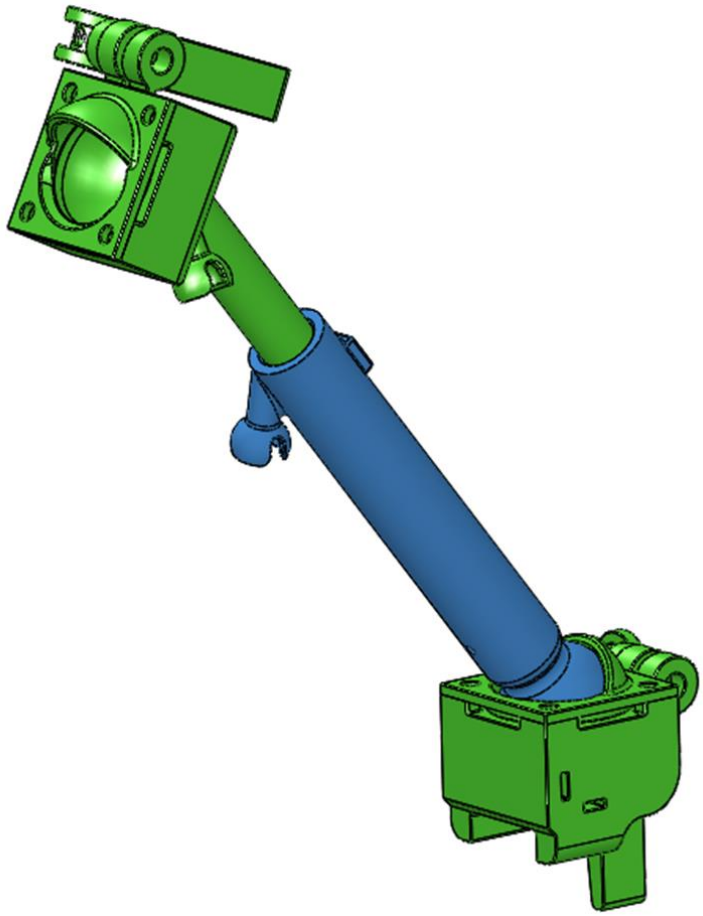

Fig. 21. EEMG support structure main shaft assembly, highlighting the lower cylinder (blue).

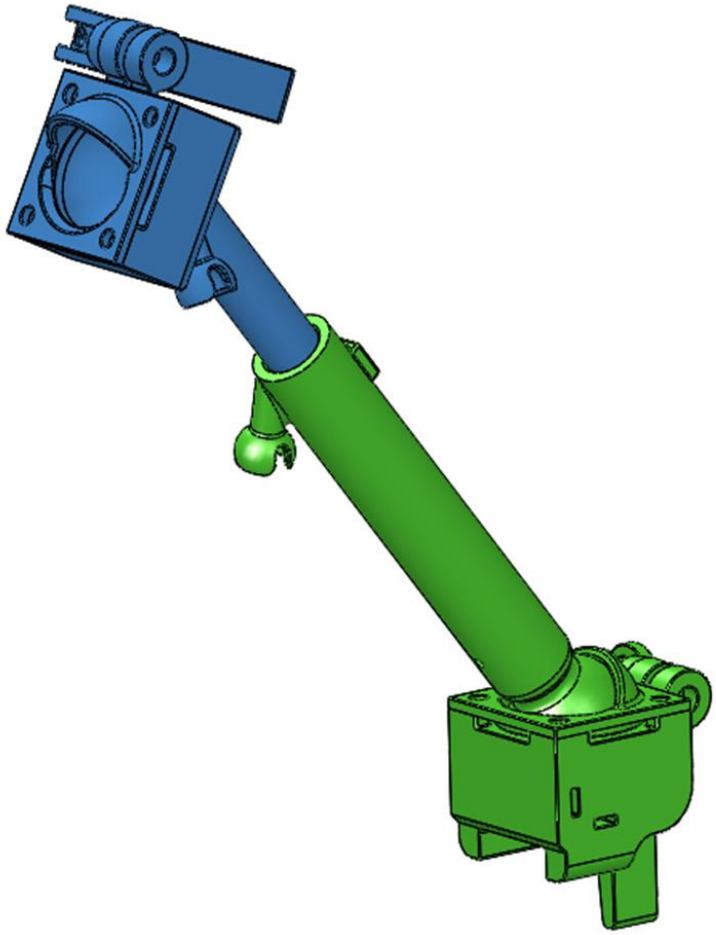

Fig. 22. EEMG support structure main shaft assembly, highlighting the upper cylinder with locking socket assembly (blue).

First, in the main shaft assembly is the lower locking socket assembly. It consists of several subcomponents including: the socket base (1), ring (2), retention cap (3), locking cam lever (4), cam pin (5), and cam spacer (6), as seen in Fig. 23. The socket base has the lower half of a 22 mm diameter spherical socket cavity to accommodate the ball of the main shaft. The socket base groove (1-a) sits on the mouth gag frame handle just behind the thumb brace for additional moment resistance and provides the socket base the needed

clearance, so that the thumb brace does not obstruct the motion of the main shaft. For this initial prototype stage, cable ties are fed through the slots (1-b) and secured around the mouth gag frame handle and the thumb brace. The ring sits on top of the socket base directly above the lower half of the socket cavity. The ring is 2 mm thick and is split so that it can be squeezed together to secure the ball of the main shaft when the device is locked. The ring also has an angled flat on one of the two ends that are squeezed together, providing an additional 1.5 mm of ring closure to ensure the main shaft is properly secured. The 2 mm thick retention cap has the upper half of the ball socket and sits on top of the socket base risers to secure the ring and the ball of the main shaft. It has an orifice with 120° opening from the horizontal that allows the main shaft to rotate from straight up to 40° from the horizontal, and a 180° horizontal opening that allows for a 120° main shaft rotation side to side. The retention cap is held in place with four 10 mm long M3-0.5 hex bolts when they inserted into the through holes and screwed into the mating female threads of the socket base. The socket base risers also serve to provide the necessary 0.25 mm clearance for the ring to close and expand as needed. The locking cam lever hinges on the cam pin and has circular cam profile, with a 0.25 mm center offset, that is cradled by the cam spacer. When a M4-0.70 hex bolt is fed through the concentric holes

in the ring and cam spacer, and screwed into the cam pin, the toggling of the locking cam lever draws the hex bolt laterally to close the split in the ring to secure the main shaft ball and, in doing so, fix the position of the lower cylinder of the main shaft.

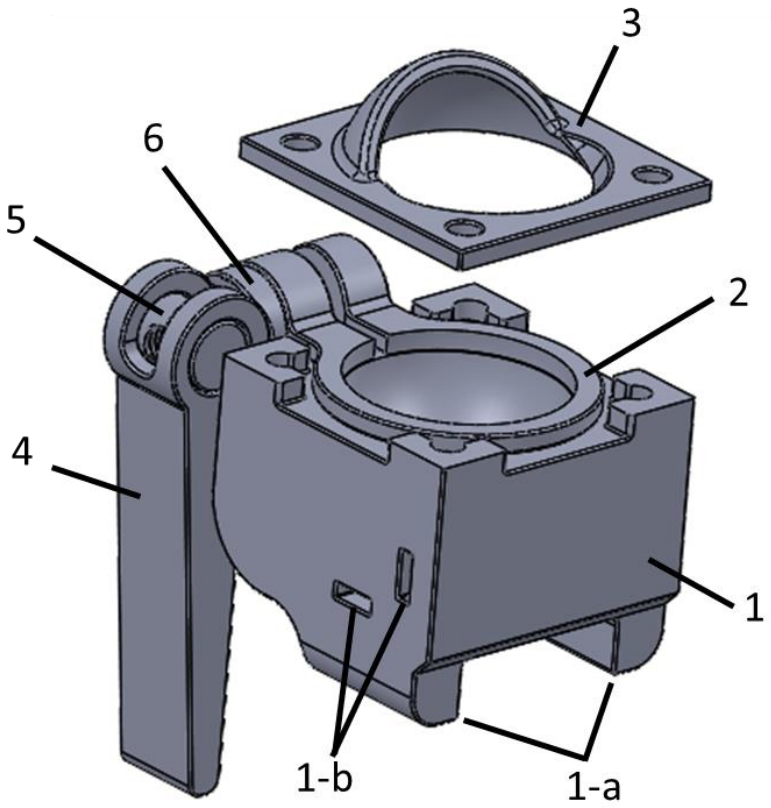

Fig. 23. EEMG support structure main shaft assembly: lower locking socket assembly with retention cap exploded for view of internal components.

Next, in the main shaft assembly is the lower cylinder as seen in Fig. 24, 25. At one end, a 22 mm diameter ball (1) rests in the lower socket assembly locking socket. It has an inner diameter of 11 mm and wall thickness of 2.5 mm. The shaft is 100 mm long from center

of ball to the distal end. Where the ball attaches to the cylinder, there is an 11 mm tapered neck (2) that increases the degree of rotation within the socket joint. Near the distal end is a square boss (3-a), 8 mm x 8 mm by 1.5 mm thick, to provide a 1.5 mm minimum wall thickness around a M5-0.80 female thread (3-b) and a screw purchase of 5 pitch lengths. The M5-0.80 female thread allows for the advancement of a thumb screw. The thumb screw tightens to provide for a friction locking mechanism to keep the upper and lower cylinders from telescoping when needed. Below the boss is the snap-fit socket to accommodate the ball of one of the secondary support members. It consists of a stem (4-a) and a socket (4-b). The 6 mm diameter stem provides separation of the socket from the lower tube, and combined with the 3mm socket slot, the socket can expand for proper ball insertion. The stem is swept back 55° towards the ball, and out 35° to align with ball-socket on front support cross-bar. The socket has an 8 mm inner diameter, same as the mating ball for a friction fit [14], 1.5 mm wall thickness, 45° chamfer to assist with ball insertion, and a 1.0 mm undercut depth. The distal tip opening of the cylinder has a 45°, 0.5 mm chamfer (5) to assist with insertion of upper cylinder.

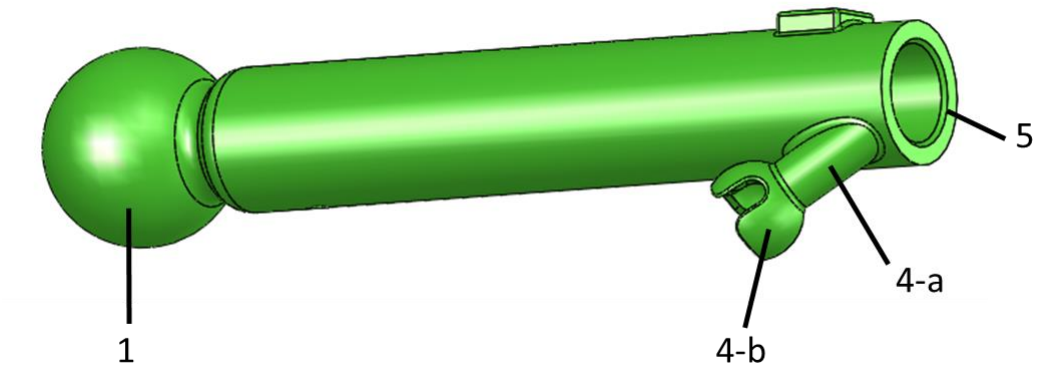

Fig. 24. EEMG support structure main shaft assembly: lower cylinder highlighting the ball, snap-fit socket stem and socket, and insertion chamfer.

Fig. 25. EEMG support structure main shaft assembly: lower cylinder highlighting the neck, thread boss, and female thread for thumb screw.

The guideline for the undercut depth (H), illustrated in Fig. 26., was calculated using Eqs. (4-6) [15]. Equation (4) defines undercut depth as it relates to the ball diameter and the socket opening diameter. This equation was substituted into Eq. (5), defining the

relation between the maximum permissible elongation and the mentioned ball-socket geometry, and algebraically solved for the socket opening diameter to produce Eq. (6). The maximum permissible elongation for materials with no distinct yield point to be used with snap joints is approximated as half the elongation at break [16]. From the material specifications of the photopolymer material, the elongation at break is 20% [17]. Given the chosen ball diameter of 8 mm, the suggested socket opening diameter was calculated to be 6.67 mm. This resulted in an undercut depth of 1.33 mm to use as a guideline and nominal value used for testing.

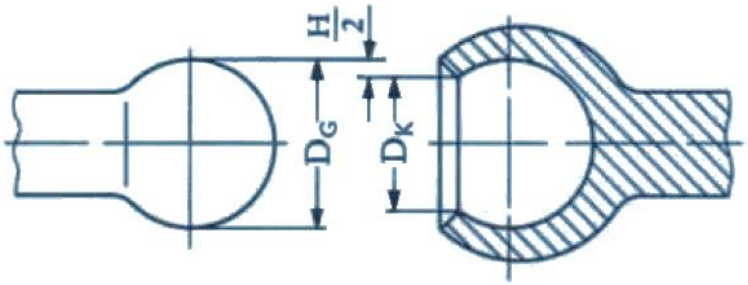

Fig. 26. Design of undercut depth of a plastic ball-socket snap-joint. Reprinted from Ticona, 2009, "Design Calculations for Snap Fit Joints in Plastic parts", http://files.engineering.com/download.aspx?folder=7fd183bb-7ac8-4891-9378-a8badd6a102d&file=Design_for_Snapfit_revi-10.pdf, "6/12/2016".

$$H = D_G - D_K \quad (4)$$

$$\varepsilon_M = \frac{H}{D_K} \cdot 100\% \quad (5)$$

$$D_K = \frac{D_G}{\left(\frac{\varepsilon_M}{100\%}+1\right)} \quad (6)$$

H = Undercut Depth

D_G = Ball Diameter

D_K = Socket Opening Diameter

ε_M = Maximum Permissible Elongation (strain)

The last section of the main shaft assembly is the upper cylinder with locking socket assembly, as seen in Fig. 27, 28. There are three main components of this section: the cylinder (1), snap-fit socket (2), and the locking socket assembly (3). The cylinder has an outer diameter of 10.75 mm, providing the 0.25mm clearance needed for the sliding fit, and a wall thickness of 3 mm. Additionally, with the nominal size of the cylinder, the 0.25 mm clearance corresponds to a RC 9 loose running fit [18]. The cylinder is 80 mm long, giving the main shaft assembly the needed extension range, while maintaining a

25 mm overlap at the forward position. The cylinder has a 3 mm wide, 0.25 mm maximum depth flat (2-a) on its top surface. This flat increases the contact area on the cylinder to help secure the cylinder with respect to the lower cylinder with the thumb screw. At the end of the cylinder opposite the upper locking socket assembly, there is a 45°, 1 mm long chamfer (2-b) to assist with insertion into the lower cylinder. The snap-fit socket is as described above in the lower cylinder. Additionally, the locking socket assembly is as described in the lower locking socket assembly without the features for attachment to the mouth gag frame. The angle between upper cylinder and the bottom surface of the upper locking socket base is 65°. This angle was chosen to provide the correct forward and rear position extension lengths when the scope holder member is in place.

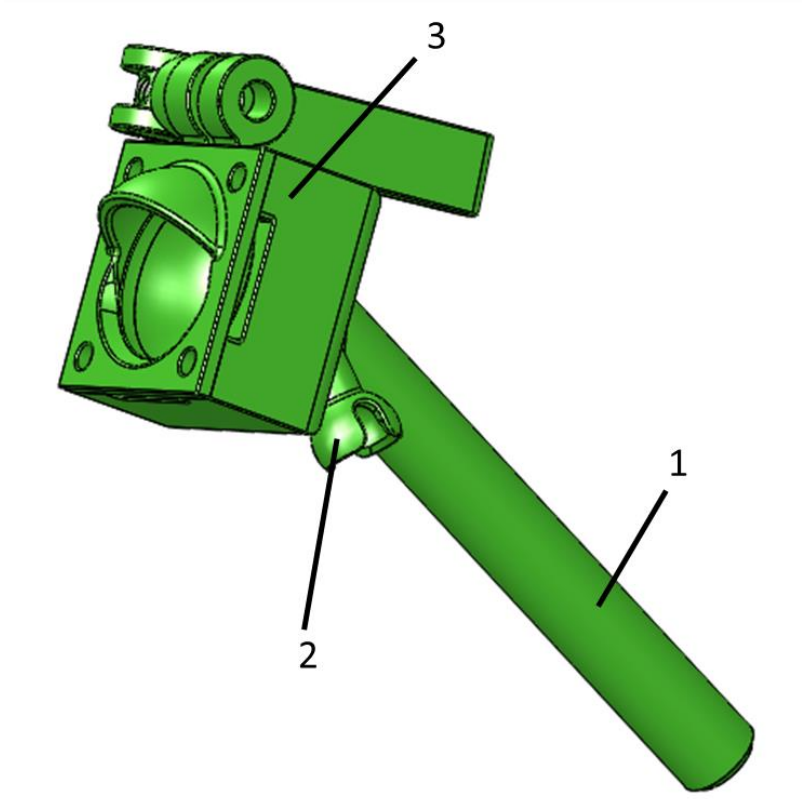

Fig. 27. EEMG support structure main shaft assembly: upper cylinder with locking socket assembly, highlighting the cylinder, snap-fit socket, and locking socket assembly.

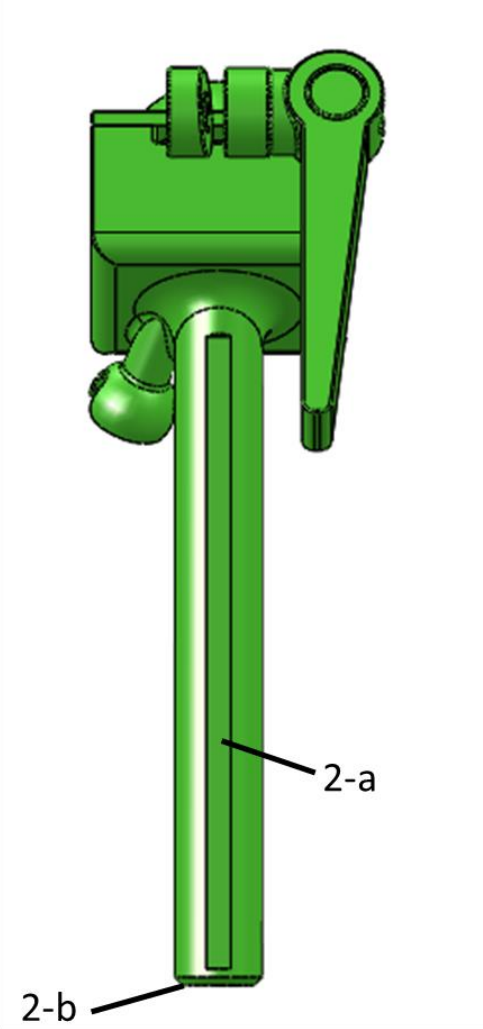

Fig. 28. EEMG support structure main shaft assembly: upper cylinder with locking socket assembly, highlighting the cylinder flat and end chamfer.

The second section of the support structure includes the two secondary support shafts, as seen if Fig. 29. These members attach to the front support cross-bar at one end and to the two snap-fit sockets on the two cylinders of the main shaft at the other to provide additional support and lateral stability for the camera/scope. Each member consists of two components: the cylinder and rod, which slide

with respect to one another, allowing for the extension and contraction of the member as the device articulates. An internal compression spring is used to provide support as the member extends and contracts.

Fig. 29. EEMG support structure secondary support shaft.

The secondary support shaft cylinder (see Fig. 30.) has an outside diameter of 11 mm and is 70 mm and from ball center to end. It has an 8 mm ball (1) to match that of the inner diameter of the socket. Similar to that of the main shaft lower cylinder, there is a 4.5 mm neck (2) to increase rotational range of motion within the socket. Near the open end is a boss 8 mm x 8 mm x 1.5 mm minimum thickness (3-a) to provide extra material around the M3-0.50 screw threads (3-b) and at least 5 pitches of screw purchase, similar to that on the main shaft lower cylinder. Additionally, there is a 45°, 0.5 mm

chamfer on the inner diameter opening (4) to assist with the insertion of the rod.

Fig. 30. EEMG support structure secondary support shaft: cylinder, highlighting the ball, neck, thread boss, female thread for set screw, and inner diameter chamfer.

The secondary support shaft rod (see Fig. 31.) has an outer diameter of 6 mm, which allows for the 0.25 mm, RC 9 loose sliding fit between it and the cylinder. The rod is 85 mm and 70 mm long from ball center to end for the long and short support shafts, respectively. The long support shaft extends up to the main shaft upper cylinder, while the short support shaft extends to the main shaft lower cylinder. The lengths of the support shaft rods and cylinders allows for an extension range of 140 mm to 100 mm and 125 mm to 88 mm for the long and short support shafts, respectively. Additionally, the rod has a 4.5 mm wide 1 mm deep flat (5-a) and a stop (5-b) at the end opposite the ball. When a M3-0.50 set screw is inserted into the

female threads on the boss of the cylinder, the stop prevents the rod from being over extended and component separation. The rod also has a 4.5 mm neck (6), similar to that of the cylinder. At the end of the rod is an 8 mm ball (7) to mate with the snap-fit sockets of the main shaft.

Fig. 31. EEMG support structure secondary support shaft: rod, highlighting the flat, set screw stop, neck, and ball.

The third section of the support structure is the front support cross-bar, as seen in Fig. 32. This member is 120 mm from end to end to provide a stable base to support the camera/scope. The arms are 7 mm wide and 10 mm tall. The base is 26.125 mm long, 15.5 mm wide, and 11.5 mm tall. The base has a 19.125 mm wide groove (1) that runs through the width to tightly fit to the mouth gag frame handle with a 0.125 mm clearance. There are two slots in this member that allow for cable ties to be inserted to secure the cross-bar to the mouth gag frame. The first slot (2-a) runs horizontally through

the cross-bar base and allows the cable tie to secure this member to the mouth gag frame handle just behind the horseshoe. The second slot (2-b) runs vertically through the cross-bar arm to secure this member to the mouth gag frame horseshoe before the bend. The cross-bar base also has a 5.5 mm rounded slot (3) to allow for the free movement of the pin of the mouth gag frame release lever as the lever is depressed. Two snap-fit sockets are centered 110 mm apart on either arm to allow for the attachment of the secondary support shafts. These sockets are as described above detailing those on the main shaft cylinders.

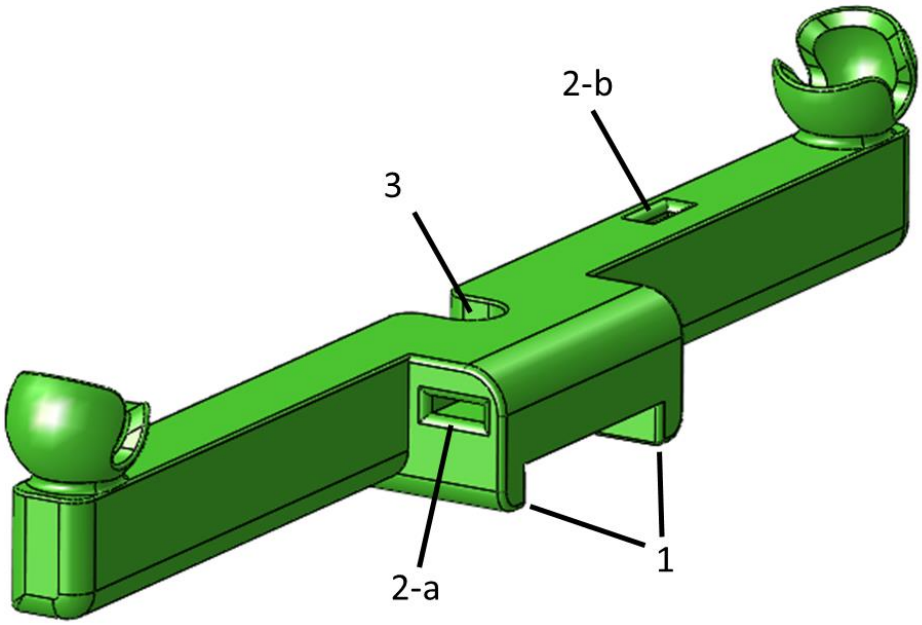

Fig. 32. EEMG support structure front support cross-bar, highlighting the cross-bar base groove, attachment slots, and clearance hole.

The last section of the support structure is the scope holder member, as seen in Fig. 33. For this prototype stage, using the 3D model of the camera/scope for reference, the scope holder member has been simplified as part of the camera/scope assembly. A 10 mm diameter, 4 mm long shaft was extended from the adapter ring that connects the camera to the scope. At the other end of this shaft is a 22 mm diameter ball to mate with the main shaft upper locking socket. The length from the center of the ring to the shaft location, when added to the shaft length and the radius of the ball, provides the 52 mm extension from the upper locking socket to the endoscope center needed for the proper forward and rear positions of the endoscope.

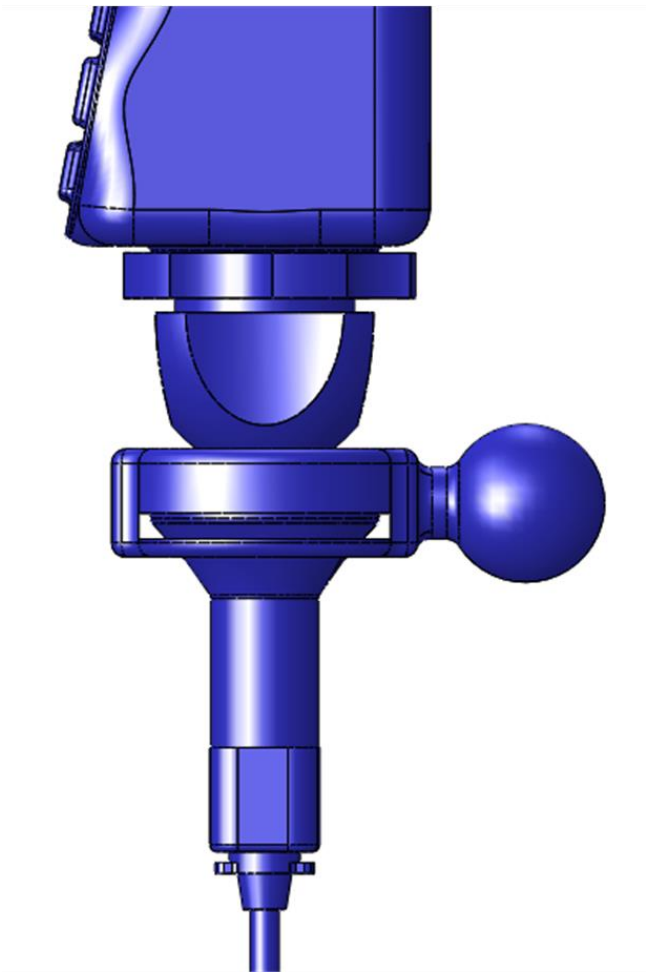

Fig. 33. EEMG support structure scope holder member connected to the adapter ring of the camera/scope assembly.

2.3.3 Testing Method and Results

In order to test device components and assemblies for proper size and range of motion, a physical model of the average patient would be necessary. An anatomical mannequin head was obtained for this purpose (see Fig. 34.). If the mannequin head's oral cavity was close in size to the dimensions measured from the scaled CT scan, it

would be valuable for design validation of physical parts. Measurements of the maximum depth, palate length (Segment A-D), and MMO were measured on the mannequin and compared to those corresponding to the CT scan (see Table 1.), and found to be relatively accurate. With an anatomical mannequin head that closely matched the dimensions of the average adenotonsillar patient, device components could be tested for fit and function with a high degree of confidence.

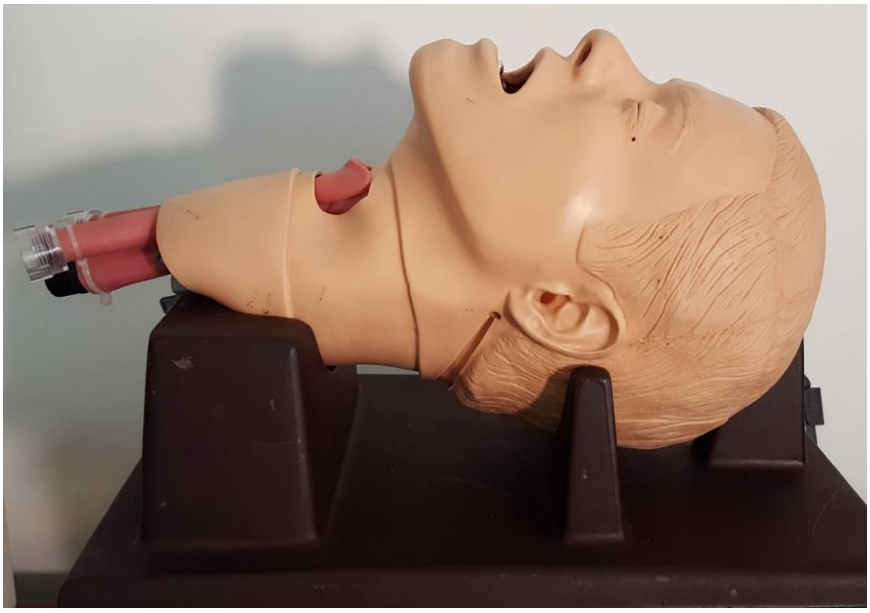

Fig. 34. Anatomical mannequin head used for prototype test fit and functionality.

Table 1. Comparison of anatomical measurements of midline sagittal view CT scan and anatomical mannequin head.

Measurement	**CT Scan**	**Mannequin**	**Δ (%)**
MMO (mm)	42	40	5
Max Depth (mm)	100	90	11
Palate Length (mm)	65	55	18

With support structure components designed and subsequently 3D printed, the components could be assembled together with the mouth gag frame, tongue blade, printed camera/scope, and anatomical mannequin head to test for fit and function. First, each component was tested with its mating parts to confirm that all fits would provide easy assembly and operation. Then the complete device (support structure, mouth gag frame, tongue blade, camera/scope, and mannequin head) to check for proper range of motion and device component function.

First, the components were tested for fit with mating parts, and no problems were encountered. Telescoping members slid with respect to each other with little force and negligible wobble. The ball of both locking ball-socket joints mated well with the upper and lower portions of the socket. The rings fit well around these balls with little force. The ball of the secondary support shafts mated well with the snap-fit sockets of the front support cross-bar and the main shaft for easy assembly and removal. All off-the-shelf hardware, including hex bolts, thumb screws, set screws, and springs fit in their orifices and through holes, and advanced well into their female threads.

Next, the complete device was assembled to test for ease of assembly, and range of motion and functionality once attached to the mannequin head. The device completely assembled with only one

issue. The problem observed was that the main shaft lower cylinder and the scope holder could not be inserted through main shaft locking socket assembly retention caps. This was easily resolved by cutting a 10 mm wide slot through the front of the cap to allow the cylinders to pass through during assembly. Once resolved and assembled, the complete device was attached to the mouth gag frame, already in place on the mannequin head, with cable ties without issue. Next, the camera/scope assembly was attached to the device as designed. With all components assembled, the scope was articulated to see if the scope tip could reach all necessary locations within the oral cavity. No issues were found as the scope was able to access all portions of the oral cavity including maximum depth, forward and rear positions, into the Nasopharynx and Oropharynx, and laterally as wide as the mouth allowed.

During the operation of the device, several issues were observed that would require design changes. First, the length of the locking ball-socket cam lever was long enough to interfere with the camera during some portions of the camera/scope articulation. Second, the scope holder shaft and main shaft were allowed to rotate a small amount about their longitudinal axes, as the ring was not sufficiently restrained from this rotation. Third, the retention cap design needed to be updated with the slot for assembly. And last, when the device

was locked in place and significant force was applied to the main shaft by hand in a back and forth motion, the ring of the lower locking ball-socket eventually broke. However, the device was able to successfully support an additional static force of two pounds when applied to the camera.

From the testing of the device on the component level and fully assembled, the first stage prototype would meet the design requirements when the retention cap was updated. The device incorporated well with the Crowe-Davis mouth gag frame. It also provided the necessary range of motion necessary to perform a surgical procedure in the Nasopharynx. And it provided the basic functionality to lock and hold the camera and endoscope in place. Although, this last requirement would need to be improved upon in the next prototype stage.

2.4 Prototype 2

The second prototype stage would have two requirements to further the progress on to the final goal of a fully functioning device. The first being to successfully address any issues that should arise during first stage testing of range of motion and functionality. The

second requirement of this prototype would be to provide features to incorporate the camera and endoscope in a removable fashion.

2.4.1 Design Changes and Rationale

For the second stage prototype, there were several design changes that were needed to be made. The first set of changes would address the issues of the main shaft locking ball-socket cam lever length, the needed retention cap slot for assembly, the ring rotation, and the ultimate ring failure identified during the stage 1 prototype testing. The second set would be to design a new scope holder member separate from the camera/scope assembly that would allow the scope to be easily removed for cleaning during surgery and replaced.

The main shaft upper locking socket lever was found to collide with the camera at some positions of camera articulation. The collision of these components interfered with the toggling of the lever into the locked position. To correct this, the original lever (45 mm from pin center to end) was shortened to 29 mm (see Fig. 35.). This would allow for the uninterrupted toggling of the lever regardless of camera position.

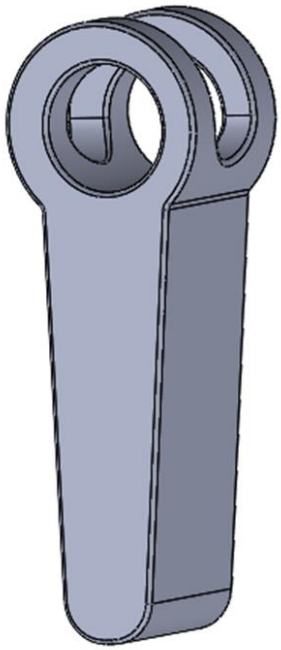

Fig. 35. EEMG support structure locking ball-socket cam lever.

The main shaft locking socket assembly retention cap was found to be missing a vital feature for the assembly of the device. The solution found to easily fix this issue was the addition of a 10 mm slot in the front of the cap, as can be seen in Fig. 36. This would allow the main shaft lower cylinder and the scope holder shaft to pass through the slot and the ball on each member could be assembled within the socket components.

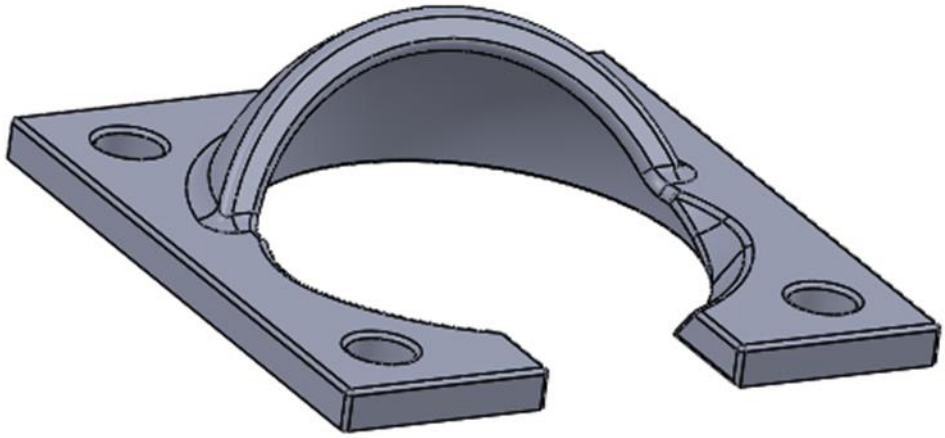

Fig. 36. Modified main shaft locking socket assembly retention cap design with slot for assembly.

The ring on the main shaft locking socket assembly was found to rotate when it was meant to be secured between the socket base and the retention cap. This allowed the ball and attached members to rotate and introduced a small wobble into the otherwise stable camera/scope positioning. This rotation was noticed when the two prongs on the ring were squeezing together by the toggling of the cam lever into the locked position. The reduced distance between the ring prongs allowed for a large tolerance between the prongs and the socket base groove where they nest. To resolve this issue a 2.75 mm wide fin was added to the socket base (see Fig. 37.). Additionally, the ring design was also modified, so that when squeezed together in the locked position, it would tighten around the fin and reduce the rotation. This was accomplished by widening the gap between ring

prongs from 1.5 mm to 3.5 mm (see Fig. 38.). Also, with the gap widened, the angled flat to allow additional travel of the ring prongs during squeezing, could be removed from the design.

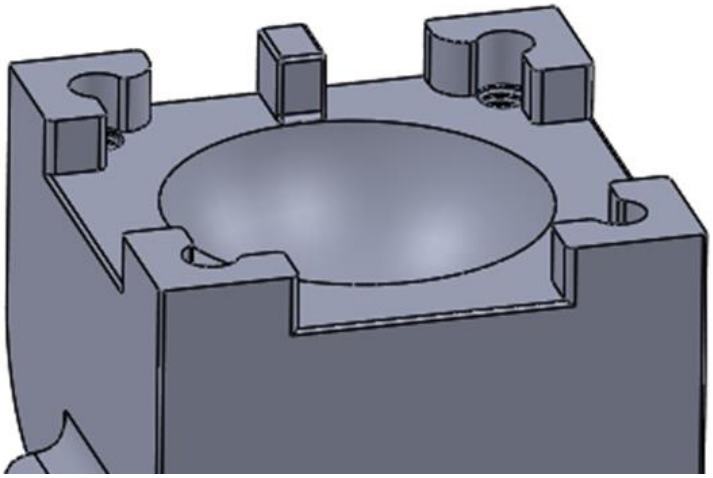

Fig. 37. Modified main shaft locking socket assembly base with added fin to prevent ring rotation.

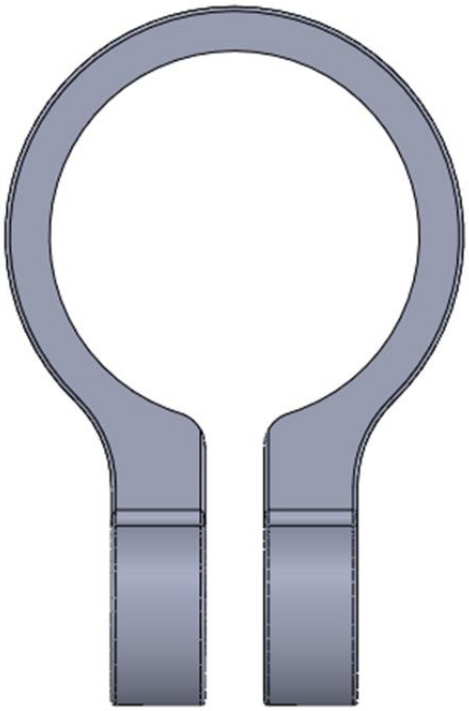

Fig. 38. Modified main shaft locking socket assembly ring with widened gap between prongs to reduce ring rotation.

During use of the assembled device, the main shaft locking socket assembly ring eventually failed during testing. The break occurred at the point where the circular profile of the ring meets the prong, as can be seen in Fig. 39 (1). Upon inspection of the ring when assembled with the socket base and lower cylinder ball, it was seen that the ring would make contact at the interior ring corners (2), which acted as a fulcrum. This pivoting action was observed to locally strain the ring at (1). To resolve this issue several design changes were made to strengthen the ring. First, the ring thickness was increased from 2 mm to 3 mm. Second, the interior corners (2) were replaced

with 2 mm fillets to reduce pivoting. And third, the outer fillet near the break location (1) was increased from 4 mm to 7 mm.

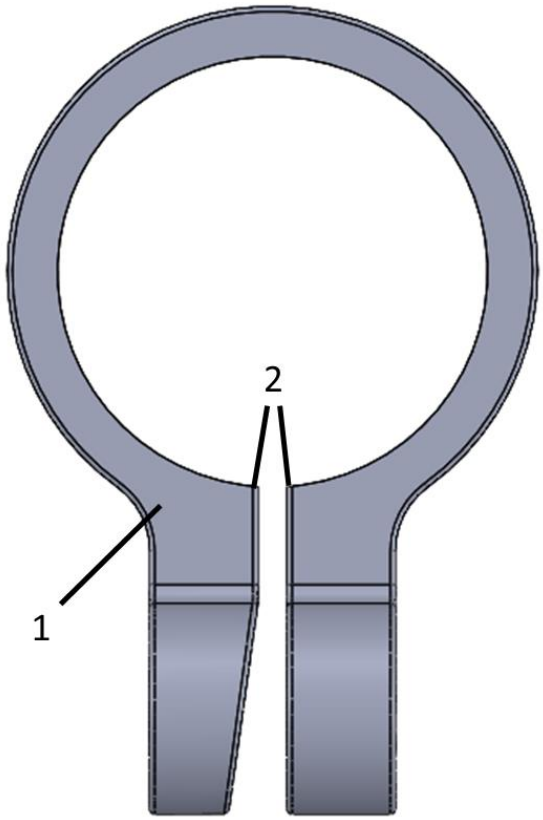

Fig. 39. Original stage 1 prototype main shaft locking socket assembly ring, highlighting the location of break during testing.

Additional design requirements for the stage 2 prototype included the incorporation of a new scope holder member that would allow for the easy removal of the camera/scope. As can be seen in Fig. 40., the scope body (1) is a sturdy, stainless steel block that serves to attach the scope eye piece (2) to the scope rod (3). This

scope body was chosen as the attachment point for the scope holder, as it is robust and its square design has rounded corners concentric with the scope rod. This would allow for a secure attachment that could be removed and repositioned with great repeatability.

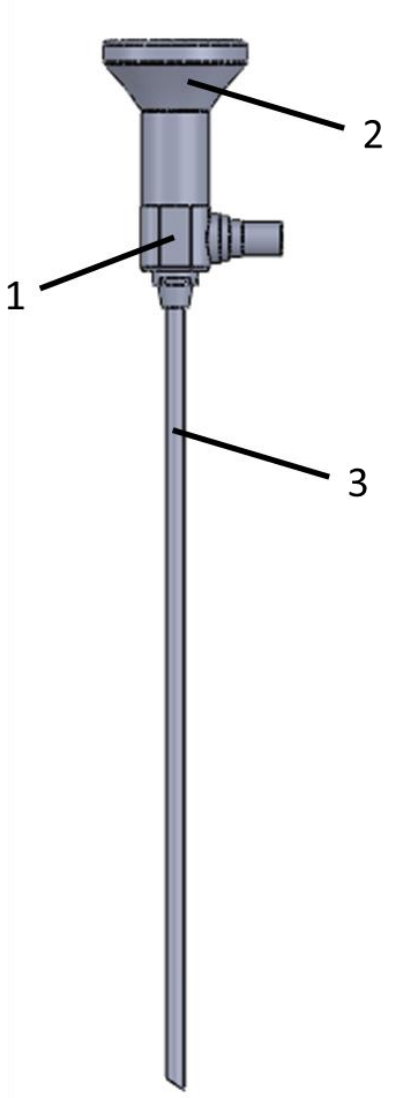

Fig. 40. Karl Storz Hopkins II, 7230-EA, 4mm diameter, 18 mm long, 120° endoscope, highlighting the scope body, eye piece, and rod.

The design of the scope holder is fairly straight forward (see Fig. 41.), as many of the dimensions were already found in the stage 1 prototype or would be determined by the scope geometry. The horizontal distance between the scope rod axis and the center of the ball was found to be 52 mm. Also, in the previous stage, the ball for the ball-socket was connected to a horizontal shaft protruding from the camera/scope adapter ring, located 27.5 mm above the center of the scope body. The new scope holder would need to have the same 52 mm horizontal distance, but drop vertically 27.5 mm from the center of the ball to attach to the center of the scope body, instead of the adapter ring. A ring would be used to secure the around the diameter of the scope, as seen in Fig. 42. (1). The scope body diameter was measured to be 17.85 mm, and using our 0.25 mm RC 9 loose sliding fit, the inner diameter of the ring would be 18.1 mm. The ring is 17 mm tall to provide full contact with the scope body for a secure fit. The ring has a cutout for the scope light source connector located on the scope body, which provides a stop for the scope once these members come in contact, as seen in Fig. 43. (2).

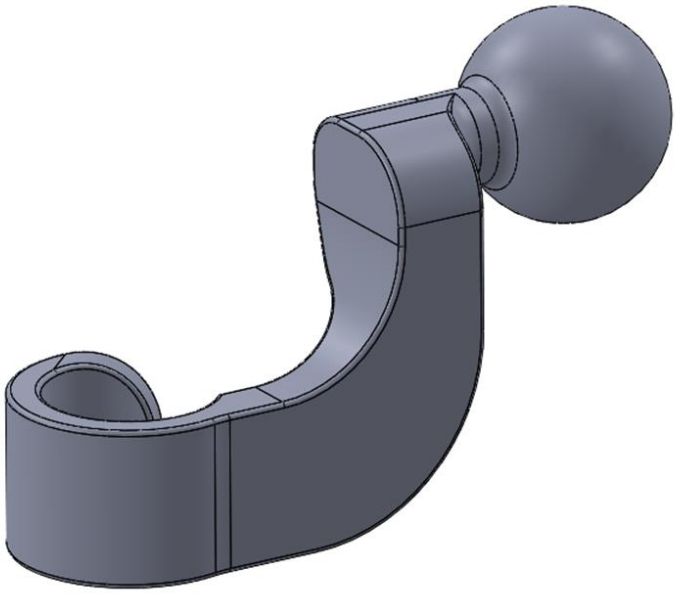

Fig. 41. Scope holder design for easy scope insertion and removal.

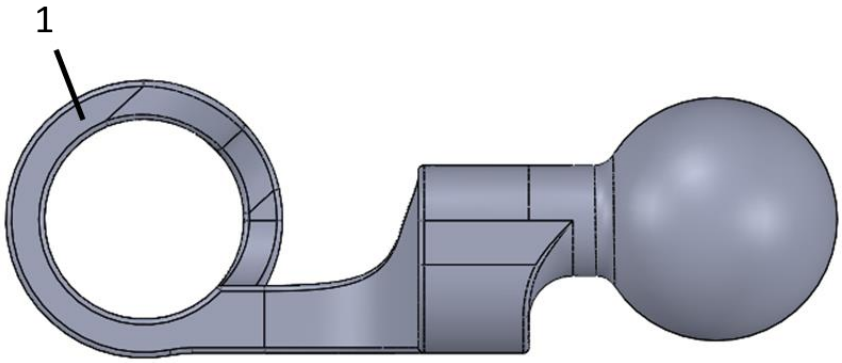

Fig. 42. Scope holder top view, highlighting scope securing ring.

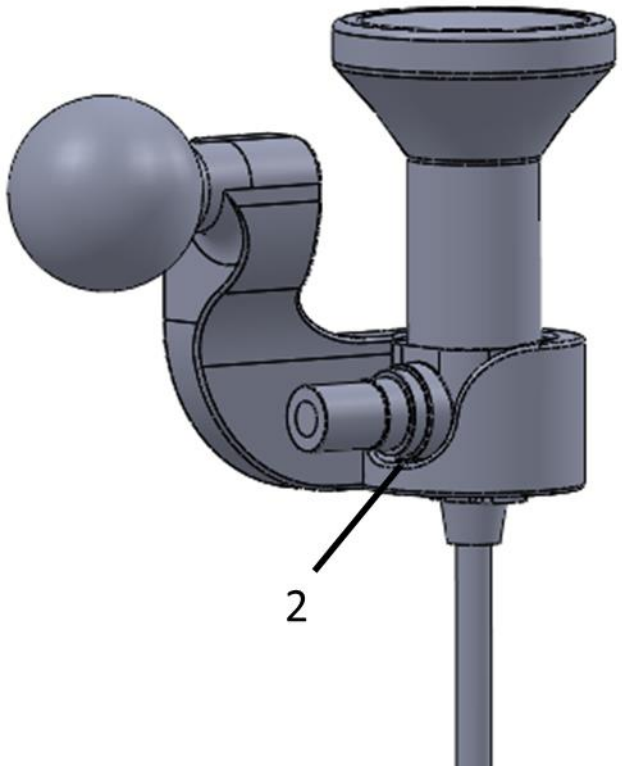

Fig. 43. Scope holder assembled with scope, highlighting the cutout to accommodate the scope light source connector.

2.4.2 Testing Methods and Results

With the stage 1 prototype testing issues addressed by the redesigned components, and the design of the separate scope holder allowing for the easy removal of the camera/scope, parts were printed and testing was conducted. The new components were tested for fit with their mating parts, and the device was assembled with the mouth gag frame on the mannequin head to test for the redesigned component functionality, as in stage 1 testing. Next, the device, with

the mouth gag frame and mannequin head, was assembled with the camera/scope and light source to test the newly designed scope holder for fit and functionality.

During testing of the newly redesigned components for fit, no issues were observed. All components fit well with the proper clearances. The slot in the retention cap provided the needed clearance for the insertion of the balls into the sockets. The ring, when squeezed together, no longer had the pivoting action, and the localized strain at the connection between the ring's circular profile and the prong was not observed.

During the testing of the device functionality with the redesigned components, no issues were observed. The main shaft locking socket assembly cam lever no longer made contact with the camera at any point in its articulation. The redesign of the main shaft locking socket base to incorporate the fin successfully prevented the rotation of the ring, removing the wobble seen in sage 1 testing. Additionally, after repeated use, no damage was observed in the ring.

During testing of the scope/camera with the newly designed scope holder, the device worked as intended, but an issue arose when the fiber optic light source was attached to the scope. The scope holder provided for the easy and quick insertion and removal of the

camera/scope. The scope holder also securely attached to the scope body. Additionally, the device fully supported the weight of the camera/scope and allowed for the proper range of motion of the scope tip. When, the fiber optic light source cable was attached to the scope body connector, due to the necessary position of the scope lens, the rigid portion of the cable interfered with the EEMG support structure, as can be seen in Fig. 44. It was found that, in order for the light source cable to not interfere with the device, the camera/scope position would have to be raised from its current position, such that the rigid portion of the cable could clear the main shaft locking socket assembly (see Fig. 45.). The distance the light source cable would have to be raised was measured to be 86.5 mm. This would require a redesign of the scope holder and also the utilization of a 30 mm endoscope instead of the proposed 20 mm endoscope. Additionally, although the scope holder could mate with any Karl Storz, Hopkins II endoscope, it would be convenient for the scope holder to be able to mate with any 4, 5, or 6 mm scope on the market. Since a redesign of the scope holder was necessary, these features would be added to the new design.

Fig. 44. Assembled EEMG device with newly designed scope holder, scope, and light source cable, highlighting the interference of the cable and the EEMG support structure.

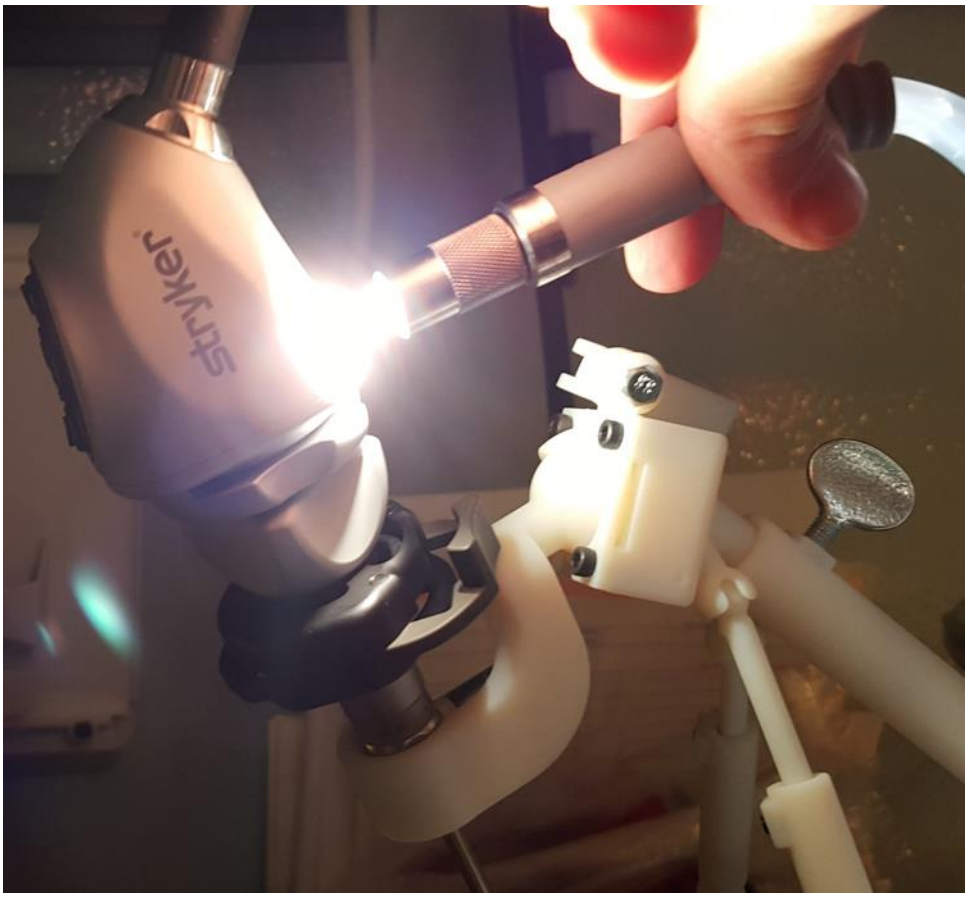

Fig. 45. Assembled EEMG device with newly designed scope holder, scope, and light source cable, highlighting the raised position of the light source cable necessary for the cable and the EEMG device not to interfere.

From the testing of the device on the component level and fully assembled, the stage 2 prototype would meet the design requirements when the retention cap was updated. All issues observed during stage 1 testing were addressed. Additionally, features were added to the prototype to provide for the incorporation of the camera/scope in a removable fashion. However, the issues with the scope holder design and the fiber optic light source cable would have to be addressed in

the stage 3 prototype, and would require a complete redesign of the scope holder member.

2.5 Prototype 3

The third prototype stage would have two requirements to be a fully functional EEMG device. The first requirement would be to address any issues that should arise during second stage testing. The second requirement of this final prototype stage would be to incorporate features that would allow the device to quickly and easily attach to the mouth gag frame. If all requirements from this prototype stage could be met, the overall goal of a fully functional EEMG device would be satisfied for this project.

2.5.1 Design Changes and Rationale

For the third prototype stage, there were several design changes that were needed to be made. The first set of changes addressed the issue of the fiber optic light source cable interfering with the EEMG support structure, and scope holder's ability to accommodate 4, 5, or 6 mm endoscopes from any manufacturer. The second set would the addition of snapping or clipping features to the front support cross-bar

and main shaft lower locking socket base, such that these members would be able to quickly and easily secure to, and detach from, the mouth gag frame.

When the assembled device was tested with the camera/scope and light source cable, it was found that the cable interfered with the EEMG support structure. The length of the scope necessitated that the cable pass directly into the secondary support shafts and into the main shaft, interfering with the operation of the device articulation. To address this issue, the location of the cable would be raised 86.5 mm to provide proper clearance of all EEMG components. The stage 2 scope holder provided a 37.5 mm vertical drop of the bottom of the light source cable connector on the scope body below the top surface of the scope holder shaft connected to the ball. Additionally, to accommodate the 4, 5, and 6 mm scopes of varying manufacturers, the scope holder would clamp to the scope rod just below the scope body components. This would allow the scope holder body to rest on the top surface of the scope holder, and provide 10 mm of the lift needed to raise the light source cable. With the 37.5 mm drop and the 10 mm lift provided by the clamp location, the new scope holder top surface would only need to be 39 mm higher than the top of its shaft connected to the ball to raise the cable to the necessary height.

The new scope holder, as seen in Fig. 46., has a neck that (1) provides the same horizontal extension as the stage 2 scope holder, and the needed 39 mm height increase to its top most surface. The scope holder has the 22 mm ball (2), as in all scope holders of previous stages. At the end of the neck opposite the ball is the scope clamp clamshell (3-a) and the scope clamp closure prongs (3-b). The closure prong, shown front, has a through hole for a M5-0.80 thumb screw, and the rear closure prong has a mating female thread. When the thumb screw is advanced, the clamp gap, as seen in Fig. 47. (3-c), closes and the clamshell secures the scope. To allow the scope holder to accommodate the three sizes of endoscope (4, 5, and 6 mm), there are three endoscope clamp profiles (3-D), top, middle, and bottom, respectively. To allow the scope to be easily inserted and removed from the clamshell, the clamp profiles were given a 0.25 mm clearance. The use of the clamp to secure the scope also allows the scope to be held at any location along the scope rod and gives another way to adjust the endoscope depth into the oral cavity.

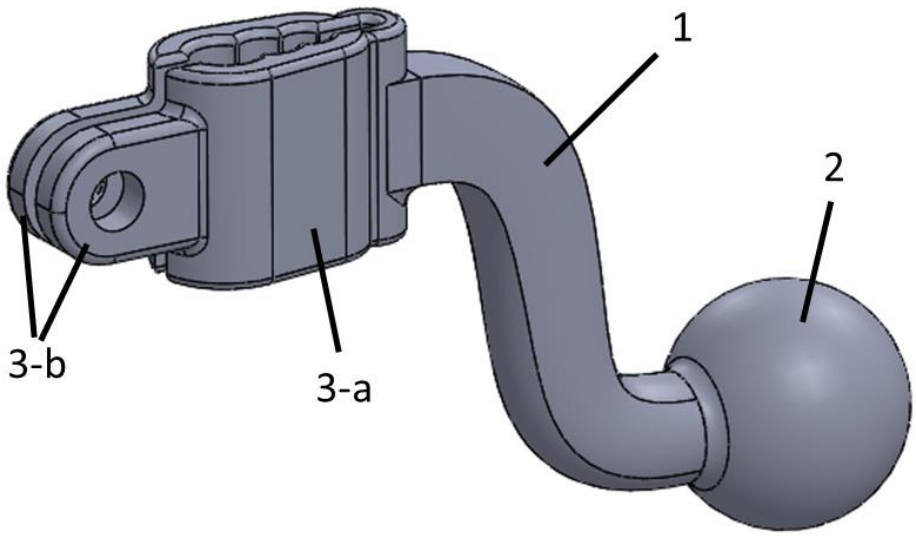

Fig. 46. Stage 3 scope holder to provide needed light source clearance, and accommodate 4, 5, and 6 mm endoscopes, highlighting the neck, ball, scope clamp clamshell, and scope clamp closure prongs.

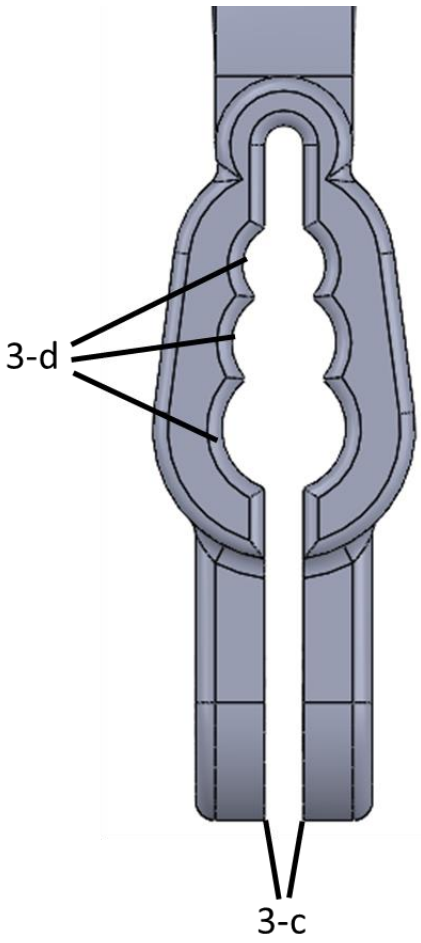

Fig. 47. Close-up of stage 3 scope holder scope clamp top view, highlighting the clamp gap and three endoscope clamp profiles.

The last requirement of this prototype stage was to add features to the main shaft lower locking socket base and the front support cross-bar to replace the cable ties used in the previous stages. These permanent features would allow for the quick and easy attachment and detachment of the support structure from the mouth gag frame.

The main shaft lower locking socket base was modified with an integrated clamp to secure the main shaft to the mouth gag frame handle (see Fig. 48.). The clamp arm (1-a) is an extension of the boss on the underside of the socket base, on one side of the slot, and extends laterally underneath the mouth gag frame handle. To tighten the clamp, a M5-0.80 thumb screw is inserted from the bottom through the through hole (1-b) and advanced into the mating female threads within the boss (2). The 0.25 mm gap between the clamp arm and the boss (2) allows for the socket base to be slipped over the tongue blade handle. The socket base can then be pushed onto the mouth gag frame handle and secured in place. The socket base can be removed by reversing the above steps.

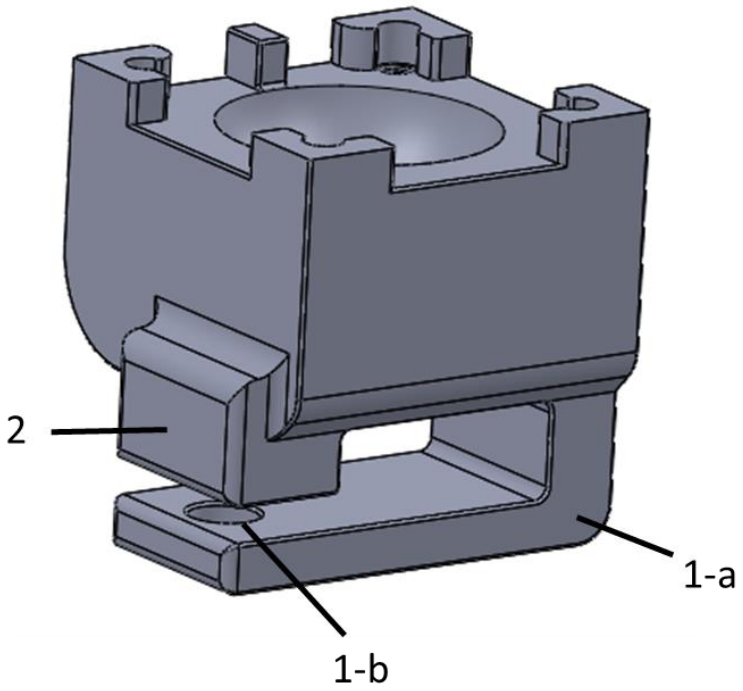

Fig. 48. Modified main shaft lower locking socket base for quick and easy attachment and detachment to the mouth gag frame handle, highlighting the clamp arm, the thumb screw through hole, and the female thread boss.

The front support cross-bar was modified to attach to the straight section of the mouth gag frame horseshoe bar and handle (see Fig. 49.). The handle hook (1) extends from the bottom side of the cross-bar and hooks horizontally to catch under the mouth gag frame handle. The horseshoe slot (2-a) sits on top of the straight section of the mouth gag frame horseshoe bar nearest the handle. The slot allows for a tight fit with the 6 mm diameter horseshoe bar with a clearance of 0.10 mm. When the cross-bar is pressed down onto the horseshoe, the snap-fit socket prongs (rear set, 2-b) snap

around the horseshoe bar to secure the cross-bar to the mouth gag frame. These sockets were designed with the same undercut as the snap-fit ball-socket joints developed in stage 1. They are 3 mm long and 2 mm wide. The cross-bar arm with the slot was able to be reduced in thickness (3 mm minimum) as it is directly supported by the steel mouth gag horseshoe bar. The cross-bar can easily be removed by pulling the end of the bar up to release the snap-fit sockets.

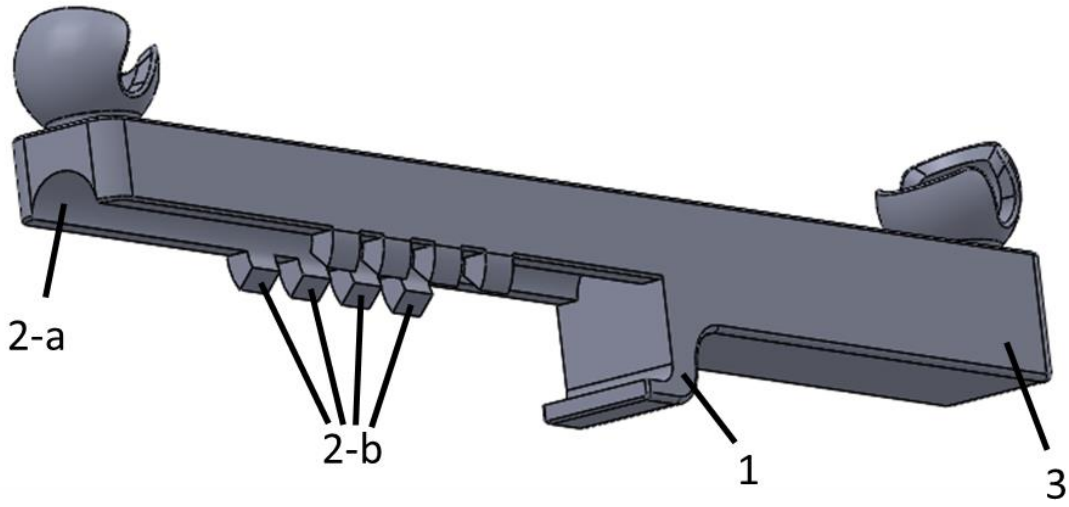

Fig. 49. Modified front support cross-bar to allow easy attachment and detachment to the mouth gag frame, highlighting the handle hook, the horseshoe slot, the snap-fit socket prongs, and the unsupported end.

2.5.2 Testing Methods and Results

With the stage 2 prototype testing issues and the accommodation of the three sizes of endoscope addressed by the redesigned scope holder, and the redesign of the front support cross-bar and main shaft lower locking socket base to be easily attachable and detachable from the mouth gag frame, parts were 3D printed and testing was conducted. Additionally, three 30 mm scope rods (4, 5, and 6 mm) were printed to be interchanged with the scope body. The EEMG components were tested for fit with mating parts, and the device was assembled with the mouth gag, mannequin head, and camera/scope to test for functionality, as is previous stages.

During testing of the newly redesigned components for fit, no issues were observed. All components fit well with the proper clearances. The 4, 5, and 6 mm scope rods slid easily into the corresponding scope holder endoscope clamp profiles. The main shaft lower locking socket slid over the tongue blade handle and onto the mouth gag frame handle with a tight fit. The front support cross-bar hooked around the mouth gag frame handle and snapped to the horseshoe bar to securely attach the cross-bar to the mouth gag frame.

During the testing of the device functionality with the redesigned components, no issues were observed. The scope holder raised the fiber optic light source cable to clear all device components. When the thumb screw was tightened the scope holder securely clamped each of the scope rods. Additionally, with the change in endoscope length, the scope was still able to reach all necessary locations and angles within the oral cavity.

From the testing of the device on the component level and fully assembled, the stage 3 prototype would meet the design requirements all design requirements. All issues observed during stage 2 testing were addressed. Additionally, features were successfully added to the prototype to provide for the quick and easy attachment and detachment of the support structure to, and from, the mouth gag frame. With the all three stage's requirements fulfilled, the EEMG device was considered fully functional.

References

1. Somendra A. et al., *Anatomy of Pharynx*, http://www.slideshare.net/AgarwalSomendra/anatomy-of-pharynx, "6/12/2016".

2. Ramos S. et al., 2013, "Tonsillectomy and Adenoidectomy", *Pediatric Clinics of North America*, **60**, 793-807.

3. Naylor, N., 1977, "Tonsillectomy and Adenoidectomy: A Review of the Literature", *Canadian Family Physician*, **23**, 113-117.

4. Bloching M. B. et al., 2007, "Disorders of the nasal valve area", *Current Topics in Otorhinolaryngology - Head and Neck Surgery*, **6**.

5. Darrow, D. et al, 2002, "Indications for Tonsillectomy and Adenoidectomy", *The Laryngoscope*, **112**, 6-10.

6. Bhattacharyya, N. et al., 2010, "Changes and consistencies in the epidemiology of pediatric adenotonsillar surgery, 1996-2006", *Otolaryngology--head and neck surgery*, **143**, 680-684.

7. Anand, V. et al, 2013, "Changing Trends in Adenoidectomy", *Indian Journal of Otolaryngology Head and Neck Surgery*, **66**, 375-380.

8. Umstaadt, L., MD, Ukatu, C., MD, Baugh, T., MD, Puricelli, M., MD, Hopewell, B., MD, 4/28/2016, Columbia, MO, "personal communication".

9. Shay, S. et al., 2016, "Patterns of Hospital Use and Regionalization of Inpatient Pediatric Adenotonsillectomy", *JAMA Otolaryngology-Head Neck Surgery*, **142**, 122-126.

10. Stratasys, *Eden 350V Brochure*, www.stratasys.com, "6/12/2016".

11. Stratasys, "PolyJet Technology", http://www.stratasys.com/3d-printers/technologies/polyjet-technology, "6/12/2016".

12. 3D-Matters, "Production Preparation Guidelines", 3dmatters.com.sg.

13. Müller et al., 2013, "Maximal mouth opening capacity: percentiles for healthy children 4–17 years of age", *Pediatric Rheumatology*, **11**, 17-23.

14. Duann, 2013, "How to Design Snap-Fit Ball Joints for 3D Printing with Shapeways", https://www.shapeways.com/blog/archives/2238-how-to-design-snap-fit-ball-joints-for-3d-printing-with-shapeways.html, "6/12/2016".

15. Ticona, 2009, "Design Calculations for Snap Fit Joints in Plastic parts", http://files.engineering.com/download.aspx?folder=7fd183bb-7ac8-4891-9378-a8badd6a102d&file=Design_for_Snapfit_revi-10.pdf, "6/12/2016".

16. Bayer MaterialScience, "Snap-Fit Joints for Plastics", http://fab.cba.mit.edu/classes/S62.12/people/vernelle.noel/Plastic_Snap_fit_design.pdf, "6/12/2016".

17. Stratasys, "FullCure Materials", http://usglobalimages.stratasys.com/Main/Files/Material_Spec_Sheets/MSS_PJ_PJMaterialsDataSheet.pdf?v=635785205440671440, "6/12/2016".

18. Oberg, E. et al, *Machinery's Handbook*, Industrial Press, Inc., New York, 618-620.